MAGISTERARBEIT

Titel der Magisterarbeit

Stability of possible Earth-like planets in multiplanetary Systems

Verfasser

Simon Rothwangl

angestrebter akademischer Grad

Magister der Naturwissenschaften (Mag.rer.nat.)

Wien, 12. März 2010

The treasures hidden in the heavens are so rich that the human mind shall never be lacking in fresh nourishment.

Johannes Kepler

II

Contents

1   Introduction

Until 20 years ago, with the first discovery of a planet in orbit around an extrasolar star, only the planets of our own system were known. The next cornerstone was the discovery of the first planet around a solar type star, 51 Peg. Since than, the number of known planets has increased drastically, more than 400 planets are known today. With these discoveries, challenges were posed onto our understanding of solar system formation. New classes of planets emerged to describe types far from what we were used to in our solar system.

Due to observational restrictions, the first years especially saw the discovery of planets of Jupiter mass or above, with the exception of planets around pulsars. However, this limit is constantly pushed towards lower masses, the goal being the discovery of planets with masses like Earth, especially in the habitable zone around a solar type star. This is an important step towards identifying the likelihood of appearance of the starting condition of life, at least as known from our home planet. The overall number of planets below one Jupiter mass today is more than 150. Of these, more than 20 have masses ten times the mass of Earth or below. The current boundaries are situated at about five Earth masses, around stars of type K. This limit will be reduced even further by current and future observational programmes and space missions.

In this thesis, the coexistence of low mass planets with more massive companions in given mulitplanetary extrasolar systems are investigated. The basic data of the systems is thereby taken from observations. Multiplanetary systems themselves are interesting, since additional bodies are exposed to perturbations by more than one object. Also, a lot data of systems with more than one planet is available, and, at least with the planet formation models used, it is likely that many systems have more than just one planet.

The aim is to investigate regions in the systems where stability of these planets is given for a long time and thus providing information whether Earth-mass objects could endure the perturbations for a long time. The two systems selected for the testing were investigated only little before, thus the general stability of test bodies was computed as well. Also, the two were chosen to be quite different, in order to provide a better study of different initial conditions. The methods used are numerical as well as analytical tools that provide information of stability, namely n-body integrations, and secular perturbation theory.

2   The systems

As mentioned, the aim in this thesis is the investigation of the stability of planets in two extrasolar planetary systems, both having more than one discovered planet. Namely, these systems are HD 60532 and HD 40307, both not well studied, especially the former. HD 60532 is situated in the constellation Puppis, harbouring two super Jupiter mass planets, while HD 40307 is located in Pictor, and has three super Earths or mini Neptunes orbiting. All planets are close to the host star, especially in the case of HD 40307. The following two subsections give a quick overview of what is published about the systems.

2.1   HD 60532

HD 60532 is a star with a mass exceeding Sun's mass, and therefore has a higher surface temperature as well, but curiously a lower metallicity. It is also quite young with only about half the age of the Sun. The planets in the system are both more massive than Jupiter, and close to the star, as mentioned above. The actual orientation of the planets inclinations with respect to the star's equator are unknown.

The two planets orbiting HD 60532 were originally found in 2008 with the HARPS search for southern extra-solar planets, which is a survey among G - K stars in the southern sky with the HARPS spectrograph at the 3.6 m ESO telescope at La Silla. The selected group of stars is based on observations of a sample starting in the year 1998 with the CORALIE spectrograph at the EULER telescope in La Silla. The stars investigated with HARPS are all rather inactive, making them interesting also for search of low mass planets, since the radial velocity changes due to the planet's motion is very low, and activity of the star is hindering the detection. Data was taken between February 2006 and May 2008, with a total of 147 spectra. Orbital solutions of these radial velocity measurements with a two Keplarian fit gave minimum masses $m\,sin\,i$ of 1.03 and 2.46 M_J. A possible 3 : 1 resonance was already suggested (Desort 2008).

In 2009, another fit was used for the RV data. The planets were assumed to be coplanar, and the inclination with respect to the plane of the sky was included as a free parameter. The best stable fit gave an i of about 20°. Also, the new fit provided a 3 : 1 resonance as well, and the stability given is for at least Gyr time scale, as long as the inclination is in the range 15°≤ 90° (Laskar & Correia 2009).

The following basic data was given about the system (Schneider 2009 and Süli et al. 2009). Note that the inclination is given with respect to the plane of the sky.

HD 60532 - Star	
Distance [pc]	25.7
Spectral Type	F6 IV-V
Apparent Magnitude V	4.45
Mass [$M_\odot$]	1.44($^{+0.03}_{-0.1}$)
Age [Gyr]	2.7($\pm$0.1)
Effective Temperature [K]	6095
Right Asc. Coord. (Eq. 2000)	07 34 03
Decl. Coord. (Eq. 2000)	-22 17 46

HD 60532 - Planet	b	c
Discovered in	2008	2008
Mass [M_J]	3.15	7.46
Semi-major axis [AU]	0.77	1.58
Orbital period [d]	201.83 ($\pm$ 0.14)	607.06 ($\pm$ 2.1)
Eccentricity	0.278 ($\pm$ 0.006)	0.038 ($\pm$ 0.008)
ω [°]	352.83 ($\pm$ 1.05)	119.49($\pm$ 9.14)
T_{peri} (JD 2.400.000)	54000	54000
Inclination [°]	$\sim$ 20	$\sim$ 20

3

2.2   HD 40307

HD 40307 is a star with a mass smaller than Sun's. The triple planetary system planets are also very low mass compared with the other known extrasolar planets, with HD 40307b the planet with the lowest mass around a solar type star observed with the radial velocity method at the time of its detection. Interestingly, the orbits are circular, or at least only very slightly eccentric. It is still discussed whether the planets are super Earths or mini Neptunes.

HD 40307 itself is a rather low mass star of type K2.5 V, with a mass of 0.77 ± 0.05 $M_\odot$. It is also rather poor in metallicity, with $[Fe/H] = -0.31 \pm 0.03$. The attached planets b, c and d were detected with HARPS in a total of 135 measurement. The rms of the radial velocity curve is 2.94 ms^{-1}, which is well above all noise. The planets masses range from roughly 5 to 10 $M_\oplus$. The periods are all less than 30 days (Mayor, Udry et al. 2009). Ratios of the periods $\frac{P_c}{P_b} \simeq 2$ and $\frac{P_c}{P_b} \simeq 2$, which would allow Laplace resonances. The data obtained is the following (Schneider 2009b and Holmberg 2007):

HD 40307 - Star	
Distance [pc]	12.8 ($\pm$1)
Spectral Type	K2.5 V
Apparent Magnitude V	7.17
Apparent Magnitude H	4.97
Apparent Magnitude J	5.41
Apparent Magnitude K	4.79
Mass $[M_\odot]$	$0.75(^{+0.03}_{-0.04})$
Effective Temperature [K]	4977 ($\pm$ 59)
Metallicity [Fe/H]	-0.31 ($\pm$ 0.03)
Right Asc. Coord. (Eq. 2000)	05 54 04
Decl. Coord. (Eq. 2000)	-60 01 24

HD 40307 - Planet	b	c	d
Discovered in	2008	2008	2008
Mass $[M_J]$	0.0132	0.0216	0.0288
Semi-major axis [AU]	0.047	0.081	0.134
Orbital period [d]	4.31 ($\pm$ 0.0006)	9.62 ($\pm$ 0.02)	20.46 ($\pm$ 0.01)
Eccentricity	0	0	0
T_{maxVR} (JD 2.400.000)	54562.77 ($\pm$ 0.08)	54551.53 ($\pm$ 0.15)	54532.42 ($\pm$ 0.2)

Barnes et al. (2009) investigated whether the planets of this system are gaseous or rocky, as well as dynamical properties. According to his paper, the initial zero value of the eccentricities would grow and interaction would keep them above slightly zero. If they were on the other hand non zero in the beginning, interaction would cause them to remain below 0.1 or even lower, but the lower the momentarily eccentricities, the older the system, especially for rocky planets. Eccentricity could also not have placed planet b into a 2 : 1 resonance with c, because this would lead to instability of the whole system. This diminishes the chance of a Laplace resonance of 1 : 2 : 4 in the system, which was also suggested unlikely by Mayor (2009).

With an assumption for the planets' radii, also the heat fluxes were calculated to be between Earth's and Io's. However, short term variations of the eccentricities in the non zero starting case would lead to heat fluxes of planet b reaching several times that of Io. In contrast, minimum eccentricities would provide values much lower.

For the planets to be rocky, formation of at least one planet had to take place inside the 2 : 1 resonance and with moderate eccentricity, which would require an unlikely amount of mass in the protoplanetary disk, even more since HD 40307 is a rather low metallicity star, or the system must be young. Considering the planets to be mini Neptunes would simplify the formation and evolution, since the resonance crossing would not have been necessary, nor is the tidal heat as high as in rocky planets. Formation could have taken place further outside with the planets migrating inwards subsequently. In this case, constrains must be made to the mass of planet b, since a too high mass would again lead to resonance, causing highly inclined orbits. Yet another possibility is that planet b started as mini Neptune and lost its atmosphere due to evaporation, leaving the core in its current place. Evaporation could take place on a Gyr time scale.

This is what is already known of the systems, and forms the basic paramters of the numerical and analytical tests performed by the author during the course of this master thesis, presented in the next sections.

3 Stability analysis

The analysis of the stability of the Earth-like planets were performed by numerical Lie integration. This integrator was developed by A. Hanslmeier and R. Dvorak, based on work done by W. Gröbner. The advantage of this integrator is that the stepsize can be adjusted easily, making it a very fast integrator, but with a high accuracy when needed. The accuracy can also be customised by number of Lie terms used. For more information see Hanslmeier & Dvorak (1984) and Dvorak et al. (2005).

The usual integration time with the Lie integrator was set with 10^6 years, although in some cases a shorter time can occur. This specific time interval was chosen due to its balance between CPU time usage and information value, since in this time frame a planet in the position of Mercury would orbit the sun about $4 \cdot 10^6$ times and a planet with the semi-major axis of Uranus would still make about 12000 orbits. This counts even more for the investigated systems, since all the planets have only small semi-major axes, with HD 60532c having the largest with 1.58 AU. The furthest test bodies were thus placed at a distance of about 15 AU, giving them about 17000 orbits in the integration time. Note also that the star is considered to be a point mass object. However, before the test objects, the given systems themselves had to be analysed.

3.1   HD 60532 - Stability of the massive planets

For the stability test of the HD 60532 planetary system, the two massive planets were integrated for a period of 10^7 years. The mutual interaction is quite significant, which can be seen in the broadening of the planets' orbits, with the inner planet having a deviation of around 0.02 AU, the outer about 0.04 AU. The movements of the planets stick to this range continuously for the whole integration period. Both planets affect each others eccentricity e as well. Especially the eccentricity of the outer planet is elevated. Although it changes over a quite broad area between 0.00 and 0.19, it is mainly centred to the area of 0.09, while planet b's changes between 0.03 and 0.37, centred in the area between 0.23 to 0.3. A slight coupling is visible, which will be discussed in section 4.4. Inclination i of both objects stays the same over time, as does the longitude of the ascending node Ω, which is expected, since both planets have the same starting values in both i and Ω. There is a constant change of the argument of the perihelion ω, and therefore of the perihelion itself, which covers all the area between 0 and 360 degrees.

In a test with little differences in initial values of i and Ω of both planets the results are changed. In this test, the difference in i is one degree, while in Ω it is 10 degrees, and integration time is longer with 68 million years. Compared to the test above, semi-major axis a, and ω behave the same way as mentioned above. Big changes are in eccentricity; in the first 8 million years, both planets show only little variation, but after that, variations increase fast. The less massive inner planet experiences drastic changes in i, with values between 3 and 13 degrees. The inner planet is also affected, although on a smaller scale. The variations range from about zero to five degrees, and coupling is visible again. The behaviour of Ω is interesting as well. While in the first 7 million years both planets librate, with planet b again on a larger scale than planet c, the less massive planet's Ω starts rotating after this time and keeps doing that until the end, with only one small pause where it resumes librating again, at around 15 million years. Planet c on the other hand keeps librating even after 7 million years, although on a larger scale as before. At about 18 million years, it starts rotating as well, but soon librates again. Until the end of the integration Ω keeps changing between rotation and libration, but for different and varying time intervals.

Another test was performed with similar, but not same initial values as in the second test. Differences between values however were the same, but with a shorter integration time of 13 million years. The behaviour in semi-major axis of both planets is the same as in both other integrations. Differences already appeared in eccentricity, where the amplitude of the variation of the eccentricity is much smaller than before, for planet b Δe is about 0.07, while for c it is 0.03. Therefore, there is less mutual excitement on both particles. ω again behaves like in the other simulations and rotates. The two different initial inclinations are again excited, like in simulation two, but at a much smaller amplitude. Planet b, starting with an inclination of 1.5° finds this starting value as lower boundary, the upper being 3.1°. Planet c is varying between two and 2.5°, the starting value. Therefore, the average value of both planets is the same, and planet c's inclination is enclosed by b's during the whole integration. All movement seem very regular. Ω, again with both planets having a difference of 10°, shows the same behaviour as i, with both planets librating and c again having the smaller amplitude, between 23 and 35°, while b's is between 5 and 50°. The initial values of both planets roughly became average values, since b had a starting value of 20° and c 30°. This test proved to be the most stable of all of the three mentioned, with both planets showing only little interactions.

Additional tests were performed, but all had results similar to the ones mentioned above. The behaviour of the system seems to have chaotic features, since little changes in the tests provided rather significant changes in the outcome. Still, with the tests mentioned, the system can be considered stable. Now, with the stability of the planetary system itself given, massless test bodies can be introduced into the system. A graphical comparison of the simulations described above is given in Figures 1 and 2.
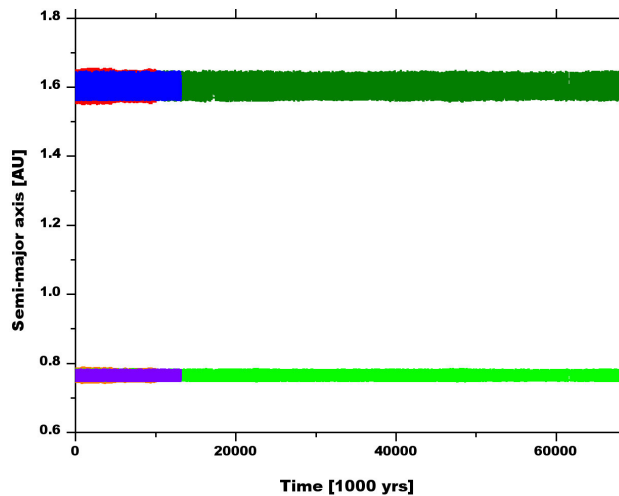
Figure 1: The behaviour of HD 60532b and c with different initial conditions in i and Ω. This plot shows the changes of a with time. The three simulations have different integration times. The colours of the two planets in the same simulations are similar, i.e. orange and red, green and olive, navy and violet.
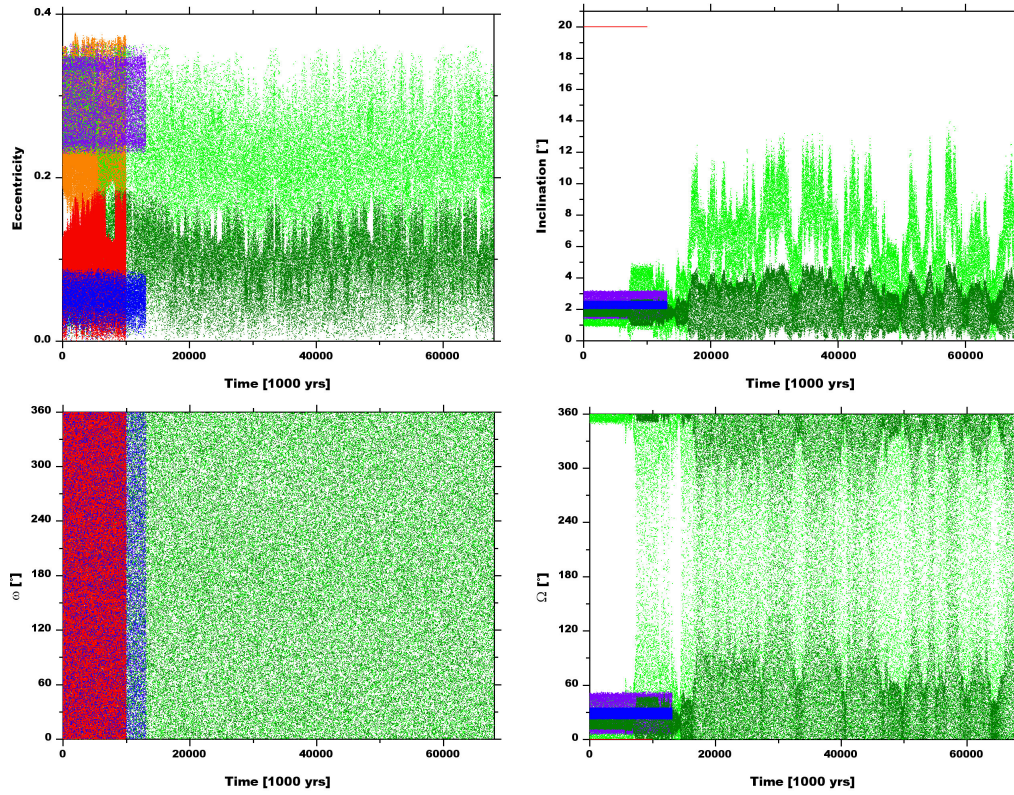
Figure 2: Behaviour of e, i, ω and Ω in the three different integrations described above. Colours are like in Fig 1.

3.2 HD 60532 - Stability analysis of test bodies

In order to investigate the stability of Earth mass planets, massless test bodies were used in the simulations. This can be explained by the mass difference between Jupiter and Earth, since the later has only little gravitational influence upon the former, so that it can be considered massless. The test bodies were distributed in three different areas, inside both massive planets, between and beyond them.

Different inclinations for the massless bodies were also tested. Most tests however were performed with an inclination of zero degrees and 20 degrees. The reference plane to the different inclinations of the test bodies, i.e. 0°, 5°, 20° and 25°, is again with respect to the plane of the sky. Thus, the test particles have inclinations of 20°, 15°, 0° and 5° with respect the the orbital plane of the two massive planets. The other initial conditions used are the following

- a is varied between about 0.1 and normally 6.0 AU, but in one case out until 14.0 AU. The step size is unregular.

- e is between 0.0 and 0.1, with a stepsize of 0.01. Sometimes, not all steps are used. The only exception are the 1:1 mean motion resonances, where also the eccentricities of the massive planets were inserted.

- ω is always set zero. Exceptions are again the mean motion resonances, where it is set to the value of the massive planets.

- Ω is also set zero almost all the time. In a few tests, it is set to a value of ten degrees.

For exact values of a and the wether the whole range of e is covered, see the tabulars in the appendix. These tabulars also show if a configuration is stable, and if not, gives the escape time.

3.2.1 Tests with 0° inclination

As mentioned before, the test was divided into three areas. First, tests were performed with objects in the range of 0.77 to 1.58 AU. In this region of the system, the massless bodies are perturbed heavily by the two massive bodies, especially since the eccentricity of the latter are increased such that planet b can have an maximum aphelion at 1.05 AU and planet c an minimum perihelion of 1.28 AU, which crosses a lot of possible orbits, and additionally comes very close to the rest. This is confirmed by the results obtained with the simulations. Of all the test objects place in this region, none is stable over the whole period of ten million years. In fact, all test bodies are removed from the system within 20000 years. The process of ejection begins immediately with increase of the eccentricity of the test particles until they reach a value close to one. The results of the integration of the systems are given in the tabular in the appendix.

The inner section of this testing, i.e. between 0.0 and 0.77 AU, is acting similar to the part between the planets, especially since the inner planets has a minimum perihelion of 0.5 AU, which again destabilises a big section. Stability is therefore only found very close to the central star, although there exists a region where the stability depends on the eccentricity of the objects.

Generally, the results are that the objects between 0.3 and 0.77 AU are removed very fast, within the first 1000 to 4000 years. Objects in a distance of 0.2 to 0.3 AU are stable for a much longer time, between 40000 and 790000 years. Interestingly, in this simulation objects with larger eccentricities are generally more stable than objects with little to no eccentricity. The planet with the longest stable phase actually has an eccentricity of 0.1.

Beginning with a semi-major axis of 0.2 AU, planets become stable. The situation however is reversed to the one in the section between 0.2 and 0.3 AU, since here planets with smaller and no eccentricity are stable. The highest stable eccentricity here is 0.6, while 0.0 is the lowest. In the range closer to the star stability of all planets increases, while the change in position between the starting point and the endpoint of the planets decreases and reaches values of almost zero percent at a distance of 0.1233 AU for all given eccentricities, which were 0.0 to 0.1. The eccentricity is also changed, with a maximum difference of 0.02 to the starting value and no object on a circular orbit any more, the smallest eccentricity being 0.01. Additionally, the objects are on strongly inclined orbits with values up to nearly 40°.

The stimulation process of the inclination is interesting; in the beginning, all planets are equally excited very fast to a value of almost 40°, followed by a phase of decrease of inclination to a value below 2°. This process is repeated continually for the first 100000 years. In the next hundred thousand years, the differences in inclination between test particles grow, leading to a less uniformed behaviour. After even more time, the differences between the particles is about 5 to 10°, so that they are distributed over all inclinations between zero and forty degrees, even though there is a slight trend towards higher values. Also, during the whole integration, the bodies constantly cover all of the before mentioned area, never reaching the boundaries of 0 or 40 degrees.

In this integration, the argument of the perihelion of the massless bodies, ω, rotates, thus reaching all values between zero and 360 degrees. That means that the perihelion is constantly changing in a rotating manner with respect to the node. The longitude of the ascending node, Ω, on the other hand is doing a libration, with boundaries being about 279 and 90 degrees. Therefore, the node is always moving in the half circle around the vernal equinox. The last-mentioned simulation is pictured in Figure 3. The tabular of the inner region in section 7.1 displays the results of the integrations.
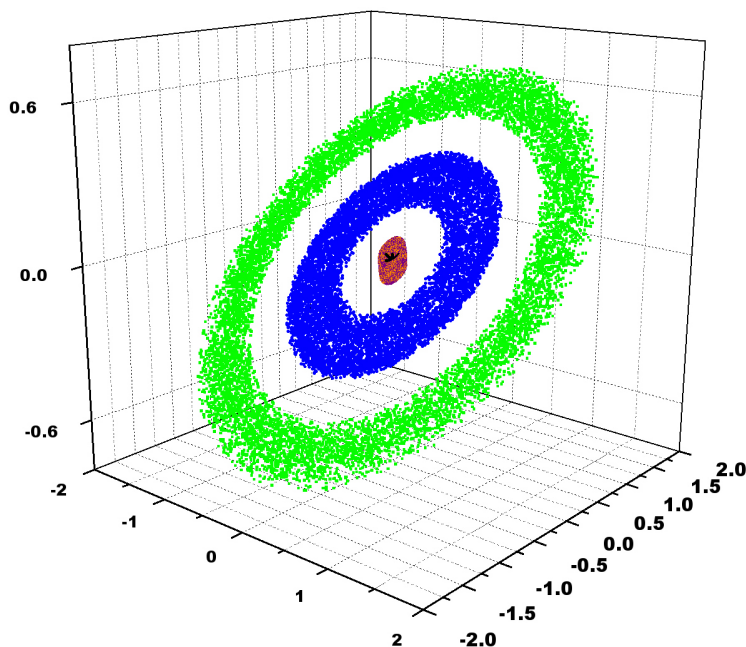
Figure 3: Massless planets at a semi-major axis of 0.1233 AU are given in multiple colours. The central star is denoted *, and is not to scale. Massive planet b is ploted in blue, c in green. Units are in AU, integration time is 10^6 years. The view from Earth is onto the x-y plane from above.

The situation outside both planets, with semi-major axes a larger than 1.58 AU is the reverse situation of the innermost part. Here, the first section is dominated by the crossing of planet c, which can have a maximum aphelion of 1.88 AU. Outwards is therefore again a zone of instability reaching to about 4 AU.

In this region of instability, the inner section is ejected very fast, within the first 5000 years. Starting at distances of about 3 AU, the ejection time increases from 30000 to 200000 years. The first stable planet for an integration time of 10^6 years is located at 3.64 AU. This planet has a low eccentricity, which is oscillating between 0.1 and 0.2, and deviation to initial value in semi-major axis is lower than 10 percent. Inclinations are excited to 0 to 45°. Both ω and Ω are librating, thus the massive planets still perturb this test body heavily. The next test configuration was placed at 3.98 AU, and again planets were stable for one million years. This time, stable planets have a higher initial eccentricity, which behaved as above. Changes in a are already as low as zero percent for the most stable planet, while for the least it is a bit above 10 percent. At 4.32 AU, only one planet is instable, also Ω is only librating, between values of 270 and 90°. The same properties are presented by planets at 4.66 AU.

Finally, all planets are stable for an integration time of 10^6 years at a semi-major axis of 5.0 AU. The deviation of these planets to their starting position is between zero and three degrees. The eccentricity is raised for all objects, with the most circular having an eccentricity of 0.057 and the most eccentric having an eccentricity of 0.29. Inclination is varying between zero and almost 40°, and in the beginning, variations are equal for all the planets involved. Later on, the phases start to differ, while the amplitudes stay the same. ω is rotating with the same frequency for all test objects in the beginning, while later, like i, the phases of the different planets change among one other. Ω is librating between values of 250 and 100 degrees. Interestingly, the libration is, like with i, in the beginning equal for all test bodies, while later the phases between them change. Planets at 6 AU act similar, only the initial eccentricities are preserved better and the phases of the different i, ω and Ω remain close for a longer time. Also, the oscillation periods are longer. Figure 4 gives a graphic of this simulation.

Finally, the 1:1 resonance was also investigated for objects with zero eccentricity and eccentricities like the massive planets. The planets were situated in the Lagrangian points L4 and L5. These places are instable as well, resulting in removal within less than 5000 years.
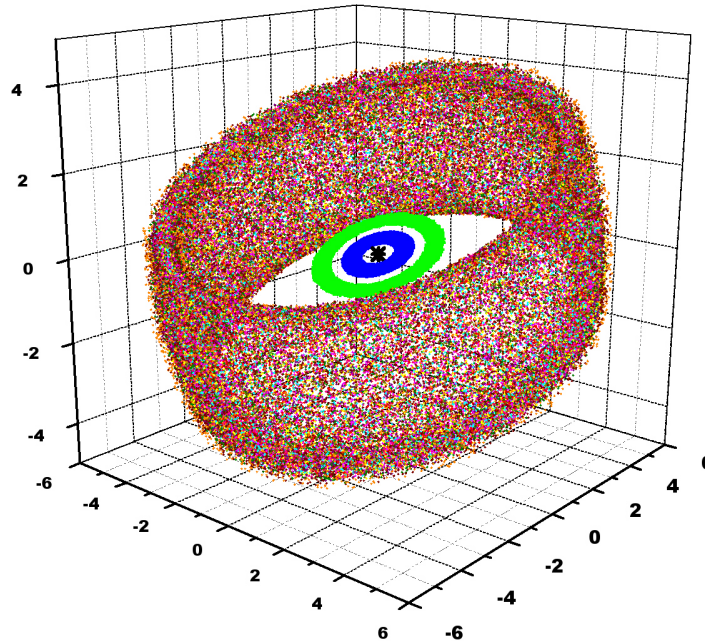
Figure 4: Massless planets at a semi-major axis of 6.0 AU are given in several colours according to their starting eccentricity. The massive planets are symbolised in green and blue. Units are in AU. Integration time is one million years.

Concluding, one could see that the tests performed with objects having an inclination of zero degrees showed the instable sections of the system quite well. Both massive planets give rise to heavy perturbations in their proximity. Only the closeness to the central star on the inside, as well as enough distance on the outside can provide stability for the test objects. The change from stable to instable orbits is performed faster on the inside than on the outside, even though some bodies showed much longer stability than other bodies in the same area. Generally, there are no big differences between initial values of eccentricity of the test bodies. Instability in this configuration is given in the section between 0.2 and 3.6 AU, although these are boundaries where not all bodies remain for the entire integration, so stability for all planets are given further in and out respectively.

Figure 5: Results of the integrations with zero degree inclination. The left graph gives an overview of all integrations, with the colour of the points according to their stability. The right graph gives a closer look to the instable zone and the borders where stability is 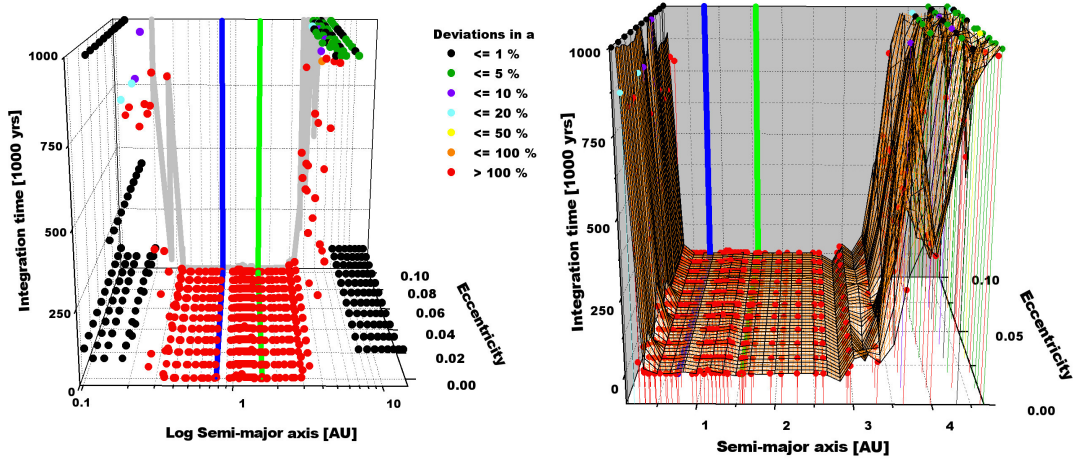again achieved. The mesh gives the approximate changes in stability. Positions of the massive planets are given by the blue and green lines.

Figures 5 to 6 give graphical representations of the results. In Fig 5, the integration time, or, in case of instability, the time of ejection, is pictured. The colour of the points represents the deviations between initial and final values in semi-major axis. Note that even though green dots indicate a change of up to 5 percent, most planets in this category have changes of three percent or less, and can therefore still be considered very stable. Instability is definitely given for all planets having a deviation of more than 20 percent. The blue and green lines mark the positions of the massive planets, while the grey graph represents the course of the integration or escape time. If, for the same initial configuration of an object, two calculations were performed with different integration times, with the shorter one stable, but the longer one not, both are given. Note also that some tests were run only for 100k or 480k years. The right graph in Fig 5 focuses on the inner, instable part. Also, in case of stability at the end, only planets with an integration time of 10^6 years are represented. The mesh gives the approximate changes in stability. Colour code of the points is the same as in the picture left. Finally, Fig 6 is a simple $\log a$ vs e plot, showing the region of instability. Finally, Table 1 shows the chance of a test particle being stable at a certain semi-major axis.
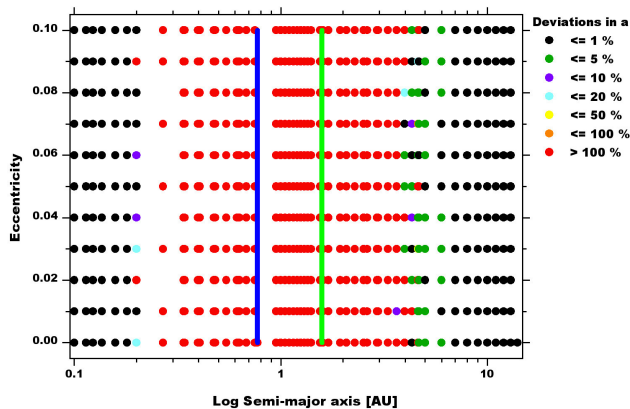
Figure 6: Stability chart that gives an overview which initial conditions of a and e are stable or instable. Colours are like in Fig 5.

	Semi-major axis [AU]						
	< 0.20	0.20	0.27 - 3.30	3.64	3.98	4.32 - 4.66	> 4.66
Lower e (0.00 - 0.05)	100	50	0	17	33	67	100
Higher e (0.06 - 0.10)	100	20	0	0	60	87	100

Table 1: Overview of how many of the test planets in a configuration are stable, in percent. Higher values mean more stability. The eccentricities are divided into lower and higher values.

3.2.2   Tests with 5° inclination

In this simulation, the test particles were placed with 5° inclination with respect to the plane of the sky, thus with 15° with respect to the orbital plane of both massive planets. The middle section of this configuration, with objects between 0.77 and 1.58 AU behaves as the one with no inclination. The escape time is below 5000 years. Again, the eccentricity of all objects increases until it reaches values of almost one.

The inner section proves to be highly instable as well, down to a semi-major axis of 0.2 AU. Here, all planets are stable for 10^6 years, although some show deviations between initial and final value of 10 to 20 percent. Also, the eccentricity changes quite drastically. For lower initial values, which is 0.00 to 0.04, the biggest change is from 0.04 to 0.26, while the lowest is from 0.02 to 0.06. For higher initial values, the changes are even higher, with values between 0.21 to 0.72.
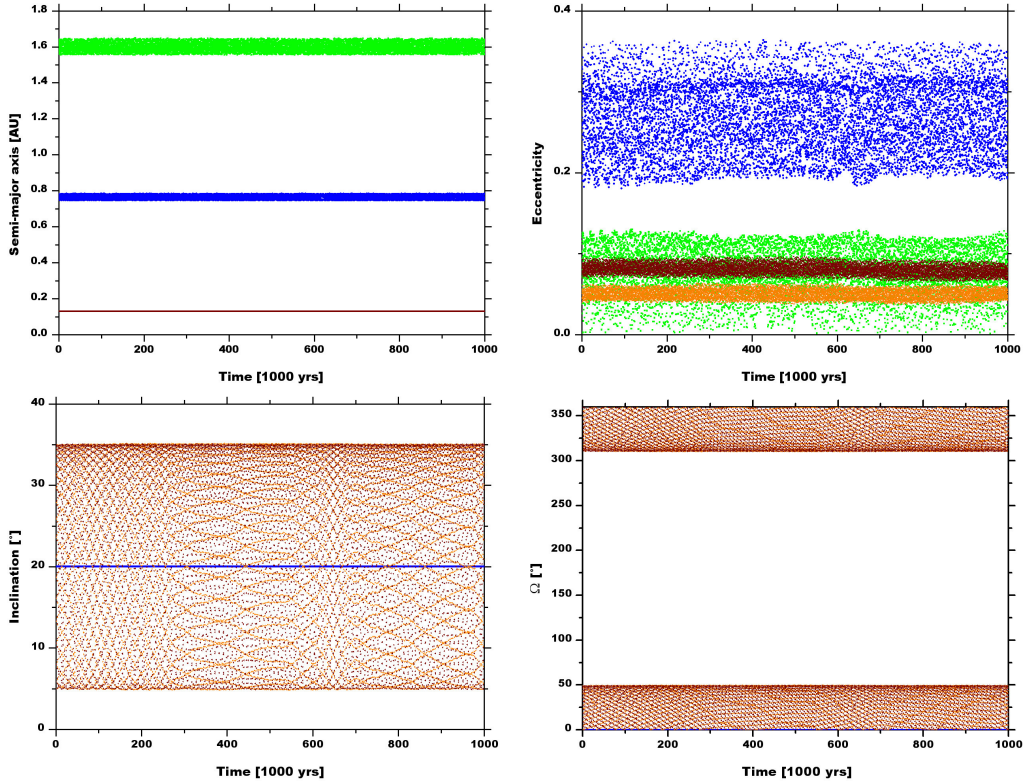
Figure 7: a, e, i and Ω of two planets at 0.13 AU with an eccentricity of 0.04 in orange, and 0.07 in wine. The massive planets are again given in blue and green.

Inclinations are increased as well, normally oscillating between 5 to 35 degrees, although in the case of the higher starting eccentricities, they can reach values of up to 45° at the end of the simulation. There also is a slight trend towards the higher end of i. ω is rotating, while Ω is librating between values of 310 and 50°, but for the higher e sample, in the end there seems to be a transformation from libration to rotation. Moving closer to the host star, the orbital deviations decrease to values close to zero at distances of 0.13 AU. Here, the eccentricity is also increased at low or high initial values, while it is almost constant at average. Inclination variates between 5 and 35 degrees. ω rotates again, while Ω librates between 310 and 50°. Of the test bodies with semi-major axes higher than 0.2, none were left in the systems after 20000 years. The behaviour of test objects is given by Fig 7.
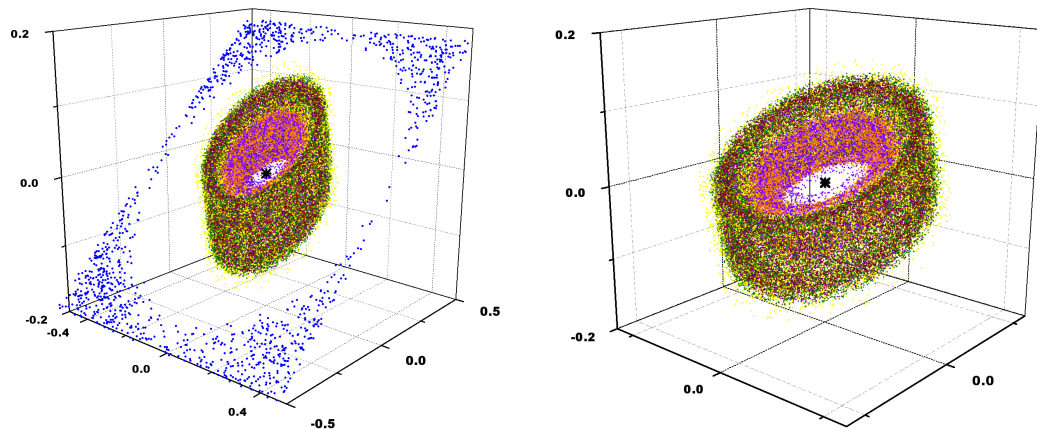
Figure 8: This graph gives test planets at two different initial a. The blue plane in the left graph is the orbital plane of massive planet b, while test bodies at 0.13 AU are coloured violet and orange. All other colours are planets at 0.2 AU. Units are again in AU.

Pictures of the inner section are given by Figure 8. In the left, the plane of massive planet b is pictured as well. Planets with a semi-major axis of 0.13 AU, with initial eccentricities 0.0 and 0.1, are violet and orange, all other colours represent planets at 0.2 AU.

Planets beyond both massive planets are instable in the first part of the section, reaching to 4.5 AU, although one planet is also stable at 3.59 AU. The stable planets at 4.5 AU have deviations of up to five percent of the starting value. Going out further decreases the deviation, there is however still a planet with a deviation of four percent at 6.0 AU. For these objects however, eccentricity stays almost constant over the whole integration period, with deviations of about 0.01. Inclination is raised to six to 30 degrees.
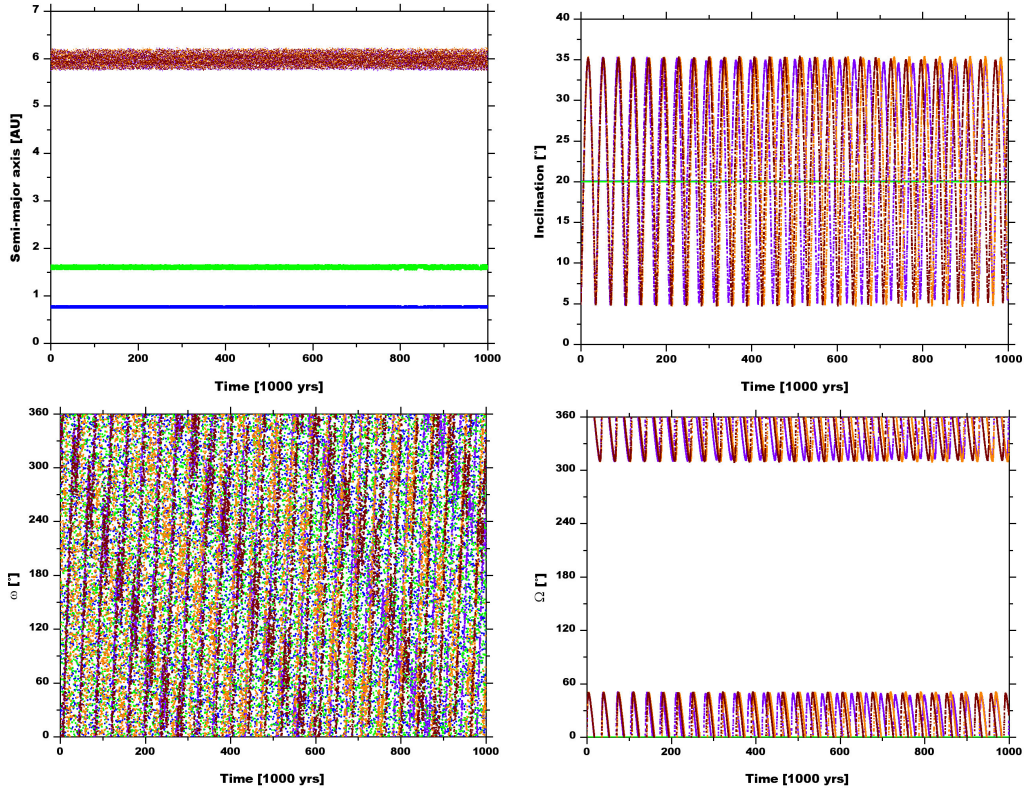
Figure 9: a, i, ω and Ω of three planets at 6.0 AU with an eccentricity of 0.00 in orange, 0.05 in wine and 0.10 in purple. The massive planets are again given in blue and green.

Figure 9 shows three planets at 6.0 AU, with eccentricities of 0.00, 0.05 and 0.10. Here, deviations are almost zero in a, while in e they are very small. Inclination again varies between 5 and 35 degrees, and all test particles show the same phase in the beginning, while they later change. The same thing happens in Ω, where oscillation is limited to the area between 310 and 50°, and ω, which rotates.

In conclusion, the instability in these tests are between 0.2 and 4.5 AU, although one planet is again stable at 3.6 AU, thus making this zone the outer boundary between stability and instability, especially since all planets at 4.5 AU are very stable. This can be seen in the local maxima in right Figure 10. The inner change between stable and instable section is again steeper than the outer. The following figures, 10 and 11 again give a graphical overview.

19
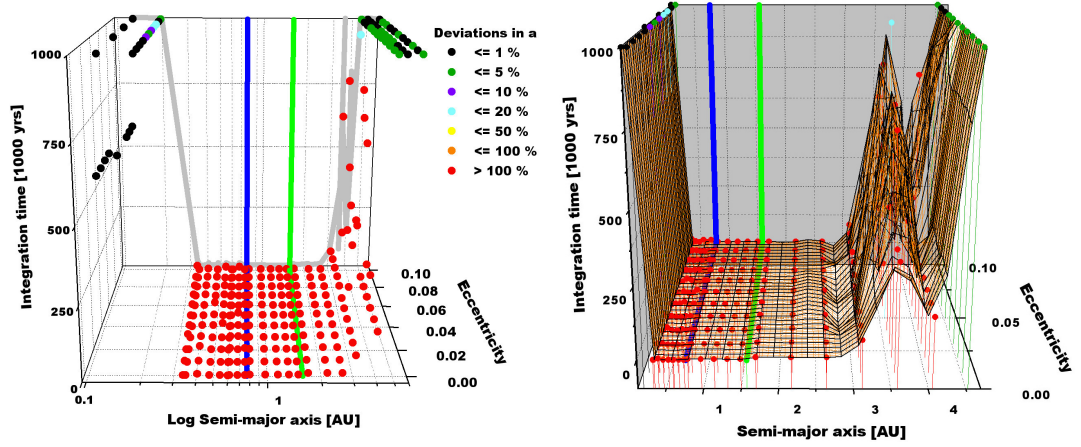
Figure 10: Results of the integrations with five degrees inclination. The left picture gives an overview of the stability and escape times of all integrations, while the right one presents a closer look onto the instable zone and the borders of stability.

The first figure gives a good impression of the variations of stability at the outer border. The wire frame in Fig 10 again gives the approximate changes between the sections. Finally, Fig 11 shows stability in a $\log a$ vs e plot. Table 2 again gives the possibility of stability in relation to a and e. The colour code again represents the deviations in a.
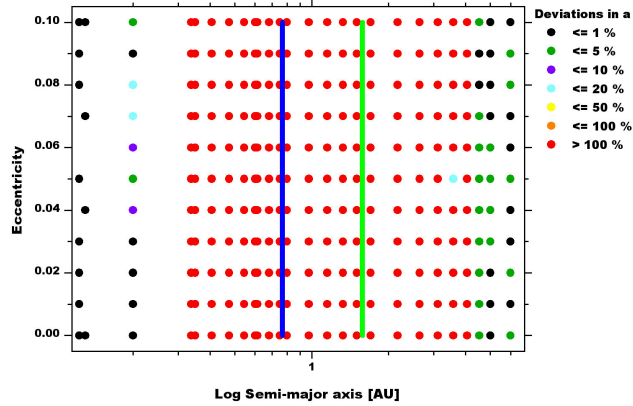
Figure 11: Stability chart.

	Semi-major axis [AU]			
	<= 0.20	0.33 - 3.12	3.58 - 4.06	> 4.06
Lower e (0.00 - 0.05)	100	0	8	100
Higher e (0.06 - 0.10)	100	0	0	100

Table 2: Overview of how many of the test planets in a configuration are stable, in percent. Higher values mean more stability. The eccentricities are divided into lower and higher values.

3.2.3   Tests with 20° inclination

In this case, the test planets are moving in the same plane as both massive planets, which makes it especially interesting. The section between both planets shows no stability again, with all objects gone after 5000 years.

More stability than the middle section is again given in the inner section. Here, again at a value of 0.2 AU, bodies with higher eccentricity are stable for the whole integration period of 10^6 years, with only little deviations of semi-major axis. The eccentricities of the stable planets are increased little in most cases, and are oscillating in two stripes; one oscillating between 0.1 and 0.2, the other between 0.05 and 0.1. Inclination is constant, and so is Ω. ω rotates again. Going to even smaller values of a, the change in semi-major axis is almost zero, as is in inclinations. Eccentricities oscillate in clearly definable boundaries, with each test particle's e separated from the others. ω and Ω behave just like above. The situation of three bodies with eccentricities of 0.03, 0.07 and 0.09 are given in Figure 12.

First stable planets in the outer section appear at 3.6 AU. The deviations in semi-major axis of the stable planets after the 10^6 year integration are four and seven percent, and eccentricities oscillate between 0.05 and 0.2. Inclinations are constant. ω is rotating, Ω is librating in a very small band. At 3.98 AU, all planets are instable again. This distance is a 4:1 mean motion resonance of planet c and the test objects. All planets except one are stable at 4.6199 AU, which is a resonance as well, namely the 5:1 with planet c. Planets in mean motion resonances will be discussed more detailed below. At 5.0 AU, all planets are stable, although changes in distance to the host star are up to 16 percent, also eccentricity is changed to values between 0.05 and 0.4. Inclination is constant, so is Ω. ω rotates, with all particles having slight differences in phase.
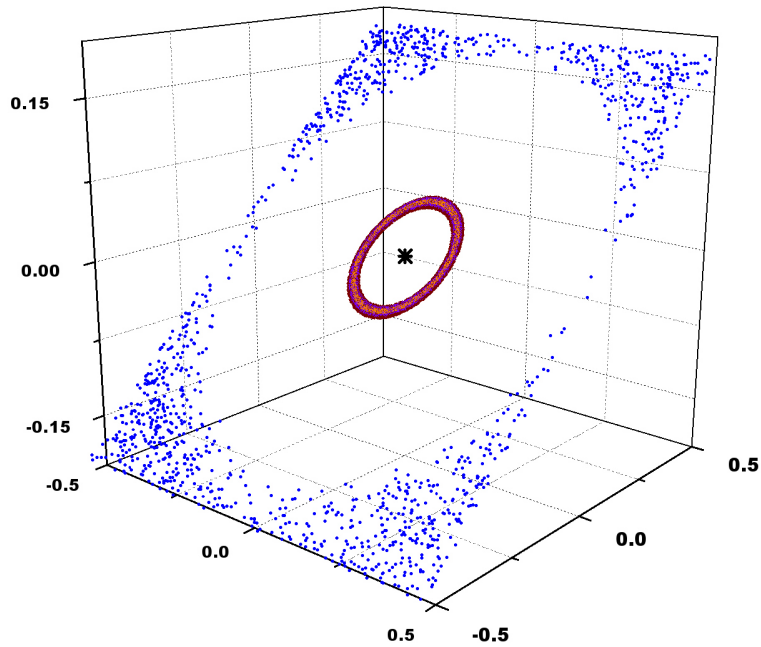
Figure 12: Zoomed on the inner section showing three planets with an *a* of 0.1233 AU, and different eccentricities. Massive plant b's orbit is given in blue. Units in AU.

At 6.0 AU, the variation in semi-major axis is down to zero to four percent, inclination is constant again. Eccentricity is between 0.0 and 0.1, with the objects oscillating between these values in a non uniform way; however, trend is towards lower *e*. *i*, Ω and ω behave as above. Fig 13 shows two of the integrations.

Finally, as mentioned above, also objects in mean motion resonances were studied, especially in a 1:1 resonance of the objects in either L4 or L5 of both massive planets. Results are also given in the table in the appendix. For both massive planets, several MMR were studied, again with varying eccentricity.
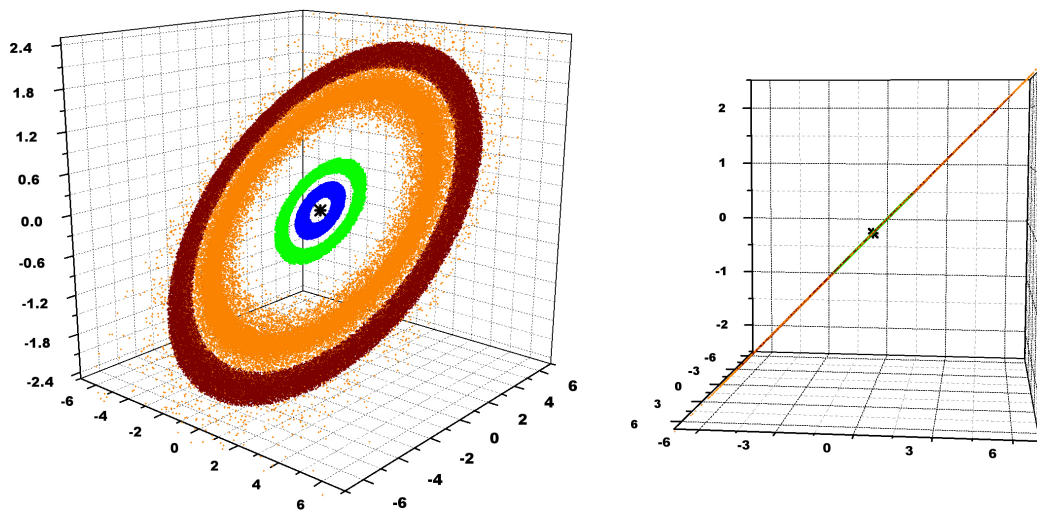
Figure 13: Left picture shows all stable planets of the tests with semi-major axes of 4.6199, in orange, and 6.0 AU, in wine. The planets at 6.0 AU are much less perturbed, as one can see. Right is the edge-on view. The massive planets are coloured green and blue. Units are in AU.

The objects in these configurations behave roughly according to the sections given above, in the way that they are only stable if they are in a stable region anyway. This however does not count for the 4:1 resonance, which is instable with ejection times of up to 490000 years, despite two stable planets on more inward orbits. All planets at 4.6199 AU, which is a 5:1 resonance of the outer planet, were stable for the whole integration time of 1000000 years, except for an eccentricity of 0.07. Objects in a 1:6 to 1:1 resonance with the more massive planet were ejected within the first 1000 years, objects with 2:1 lasted for less than 10000 years, in 3:1 for 280000 years. Still, if one considers the ejection times, it can be seen that stability increases outwards.

The test bodies in resonance with the inner planet were also placed in 1:6 to to 1:2 and 2:1 to 6:1 difference orbital period. These particles however have their orbits completely in the instable region of the planetary system, and thus are ejected. The earliest removals start at 1000 years, the longest particle lasts for 74000 years.

10 Planets in a 1:1 resonance with both massive bodies were placed into each L4 and L5, again with eccentricities from 0.0 to 0.1. However, also these bodies prove to be instable, and are ejected rapidly within the first 1000 years.

23
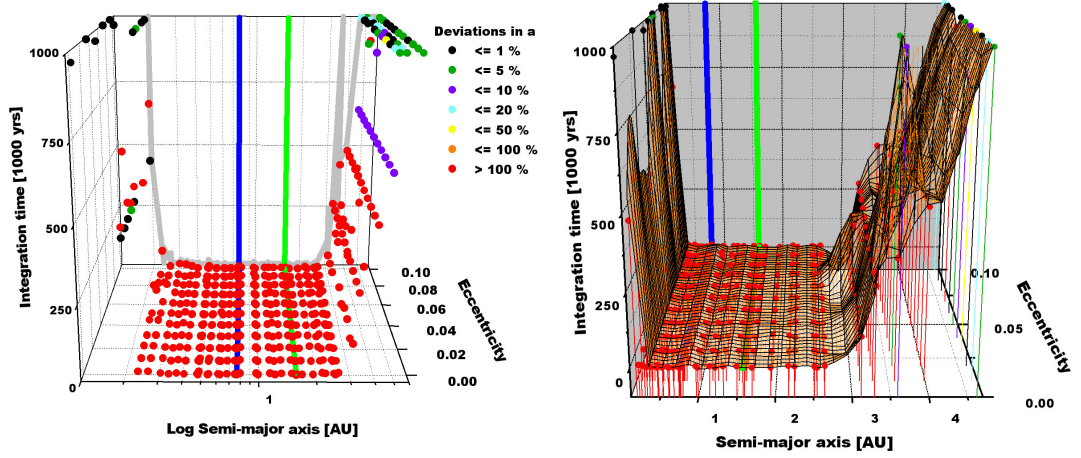
Figure 14: Results of the integrations with twenty degrees inclination. For explanations see text.

Closing, the boundaries of stability in this configuration are again given by 0.2 and 3.6 AU, but again some planets are instable at these boundaries. The gradient of the inner boundary is also much steeper than the outer one's, where again the escape times increase in a wider zone, which can be seen in Fig 14. The three figures showing the stable and instable regions are as in the sections above. Table 3 again correlates a and e with the stability.
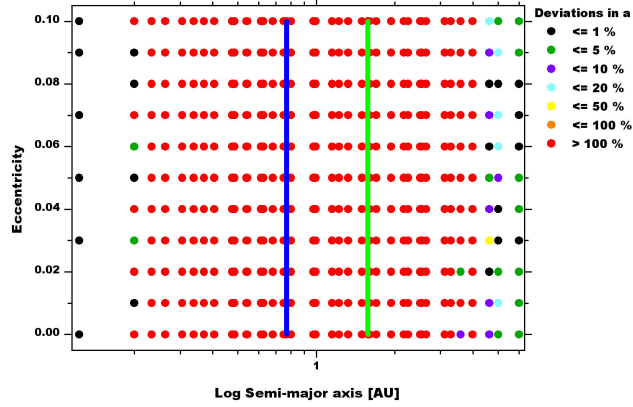
Figure 15: Stability chart.

	Semi-major axis [AU]					
	< 0.20	0.20	0.23 - 3.28	3.58 - 3.98	4.61	> 4.61
Lower e (0.00 - 0.05)	100	17	0	17	83	100
Higher e (0.06 - 0.10)	100	60	0	0	80	100

Table 3: Overview of how many of the test planets in a configuration are stable, in percent. Higher values mean more stability. The eccentricities are divided into lower and higher values.

3.2.4   Tests with 25° inclination

Last in this system, planets with 25 degrees inclination were positioned in the system. In this configuration, like in all others investigated before, no stability is found between planets b and c. The objects are removed within 5000 years.

Also, like before, 0.2 AU proves to be the barrier of stability in the system. Further out, the planets are ejected within 1000 to 30000 years. In this case, at 0.2 AU however, only two planets are stable, both with low eccentricity, and both with only little discrepancy to the initial values in semi-major axis. Eccentricity of both are moving between 0.05 and 0.2. Inclination is also changed, and is now oscillating between 15 and 25°. Ω is librating in a rather small area between 345 and 25°, while ω is rotating again. At 0.1233, all planets are stable, with almost no deviation in distance to the host star, eccentricities are between 0.01 and 0.10, with each test body oscillating in a specific band, which is separated from other's. Inclinations are oscillating again, between 15 and 24 degrees. Ω and ω show the same behaviour as with the stable plants above. The left graph in Figure 16 displays the $\log(x)$ vs $\log(y)$ situation of the stable systems above. The two planets with 0.2 AU, eccentricities 0.01 and 0.04 are in violet and wine. Of the four planets with 0.1233 AU, the difference in starting eccentricities is clearly visible, with the ones with the low eccentricities 0.0 and 0.01 pictured in orange and yellow respectively, while the ones with higher eccentricities, 0.09 and 0.10, are coloured magenta and olive. The right graph in Figure 16 shows the $\log(x)$ vs $\log(z)$ plot. Again, the planets are coloured in the same way as above. Here, the separation between the two groups of planets with different semi-major axis is not as clear as before any more, as is the situation with the two different groups in eccentricity of the system with at 0.1233 AU.
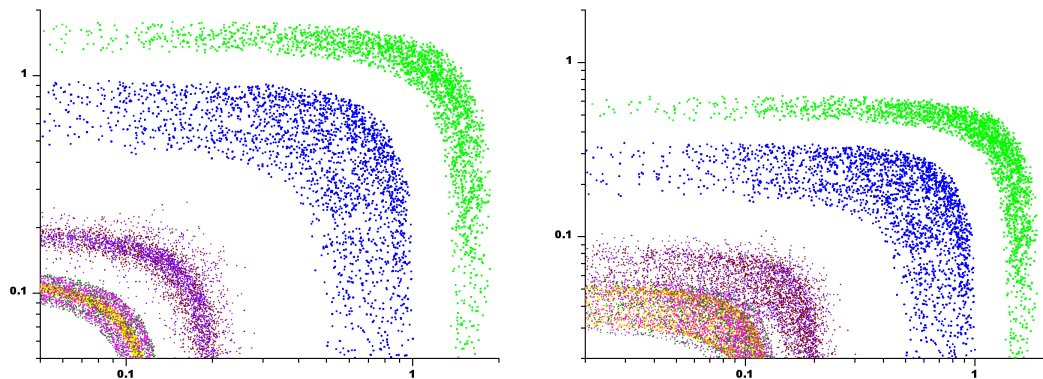
Figure 16: The left graph displays a $\log(x)$ vs $\log(y)$ plot of the stable planets of the systems with 0.2 and 0.1233 AU. The right one is a $\log(x)$ vs $\log(z)$ plot. Two planets at 0.2 AU are given in violet and wine, the four at 0.1233 AU are orange and yellow, for lower initial eccentricities, and magenta and olive for higher. The massive planets are blue and green. Units are in AU.

Outside both planets, the first stable planets in a 10^6 year integration appear at 3.586 AU, both with average eccentricities. During the integration, both eccentricities are in the area between 5 and 25°, and inclinations are moving between 15 and 25°. Ω is librating between 345 and 25°, although during testing the lower value is shifted a bit to lower degrees. ω is rotating again, and there seems to be a coupling of the rotation of all planets, at least in the beginning. Afterwards, the angles are shifted to each other. Deviations in distances are also low, having values of five and six percent. Going further outside, one planet is stable at 4.057 AU, again with average eccentricity. The outcome of the integration is similar to the one of the two planets above.

At 4.5 AU, most planets except the ones with an e of 0.07 to 0.09 are stable, although the ones with 0.06 and 0.10 eccentricity have a deviation of 8 and 11 percent respectively to the initial value. All others are between zero and one percent. The eccentricities remain between 0.01 and 0.15, and again the inclinations are oscillating between 15 and 25°. The picture at 5.0 AU is practically the same as with 4.5 AU, only the planet at an eccentricity of 0.06 is more stable.

At 5.5 AU, all planets are on regular orbits, the changes in distances are one to four percent, eccentricities are also moderate between 0.07 and 0.15, only the highest initial eccentricity is elevated to 0.24, with small variabilities in all e. Inclinations behave as before, having values of 15 to 25 degrees. Like with other initial inclinations, the oscillations have same phase and slight differences in frequencies in the beginning, therefore the phases later change. Same is for ω, where there seems to be only little differences in the frequencies, since the are aligned in the beginning, while in half the simulation they appear to be mixed, later they are aligned again. Ω is equal to i, with libration between 348 and 10°. At 6.0 AU, all variances decrease, with eccentricities of all test planets between almost zero and 0.11. i and Ω behave as with the bodies at 5.0 AU, as does ω, only here the frequencies are much closer together. Therefore, they all seem aligned during the whole integration.

Figure 17 again show the $\log(x)$ vs $\log(y)$ and $\log(x)$ vs $\log(z)$ plot. The two planets at 3.586 AU, with eccentricities of 0.04 and 0.06 are presented in violet and wine respectively, while the one at 4.057 AU with an eccentricity of 0.05 is coloured orange. Four planets at 6.0 AU are also showed, with eccentricities 0.0, 0.03, 0.07 and 0.1 are pictured in yellow, red, olive and magenta respectively. The outer system is well separated in the $\log(y)$ plot, though the difference in initial eccentricity is well visible. The two inner systems are in almost the same space. In the $\log(z)$ plot, all systems are much closer again, especially at higher z. Also, the difference in eccentricity is not as visible as before.
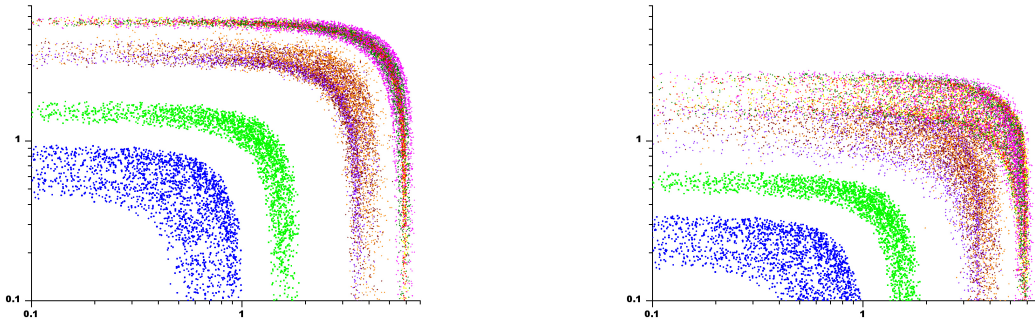
Figure 17: Left: the stable planets at 3.586, in violet and wine, 4.057, in orange, and 6.0 AU, coloured yellow and red for lower eccentricities, olive and magenta for higher, in a $\log(x)$ vs $\log(y)$. Right: the same planets in a $\log(x)$ vs $\log(z)$ plot. The massive planets are blue and green, units are in AU.
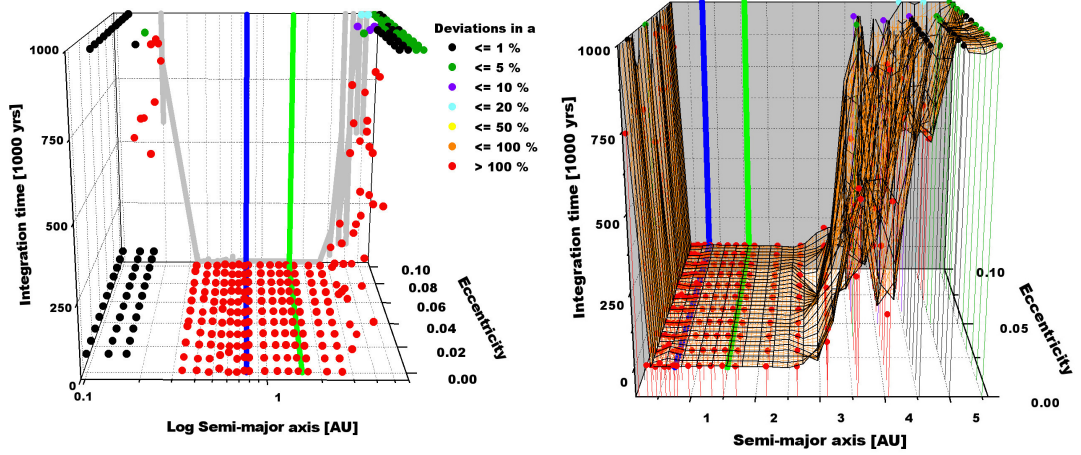
Figure 18: Results of the integrations with 25 degrees inclination.

Concluding, like in the three other configurations, the inner boundary between stability and instability is 0.2 AU. However, on the outside, objects are stable for one million years at semi-major axes of 3.6 AU. This leads to strong variations in stability and escape time in the zone between 3.0 and 5.0 AU, which can be seen in Figure 18, where in the right graph the wire frame again gives the approximate changes between data points. General stability is achieved at 5.5 AU. Table 4 compares the chances of stable orbits in relation to a and e.
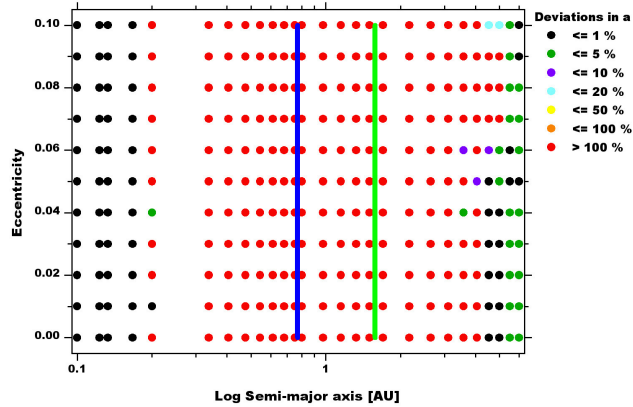
Figure 19: Stability chart.

	Semi-major axis [AU]					
	< 0.20	0.20	0.33 - 3.11	3.58 - 4.06	4.52 - 5.00	> 5.00
Lower e (0.00 - 0.05)	100	33	0	17	100	100
Higher e (0.06 - 0.10)	100	0	0	10	40	100

Table 4: Overview of how many of the test planets in a configuration are stable, in percent. Higher values mean more stability. The eccentricities are divided into lower and higher values.

Finally, the different configurations in i can be compared. Generally, all behave similar, thus there is only little dependence on inclination. All systems inner boundary of stability is 0.2 AU, although the stability of some planets provides differences. Most stability at this border is provided at an five degrees inclination, with two of the eleven data points having a deviation of 20 percent or less, while the rest is at ten or less percent. Least stability at this point is given at 25° inclination, with only two planets stable. Also, 0° inclination provides more stable results than 20°, thus lower inclinations with respect to the plane of the sky, which are higher i with respect to the plane of the massive planets, are more a bit more stable at this point.

The outer boundary is at around 3.6 AU, with all planets having at least one stable planet at this distance. 20° and 25° configurations prove to be the most stable here, with one very and one average stable planet. General stability is given outside of 4.6 AU. The variations at the outer boundary are the least for zero and 20°, although both show peaks as well, due to the stable planets. 5° shows more variations, and even stronger 25°. This means that there are big differences in escape time between the stability of the different initial eccentricities, as well as between small changes in initial semi-major axes for these systems.

3.3   HD 40307 - Stability of the massive planets

The first task in this system was again to test the stability of the system itself. As it can be seen in the data, this system is very different from HD 60532, with three relatively low mass planets in circular orbits around a rather low mass star. The planets themselves are very close to the central star, with the outermost having only about one third of the distance between Sun and Mercury.

Integration of the system for 10^6 years showed that the system is indeed very stable. The beginning values of eccentricity changed after the start to values between $6 \cdot 10^{-7}$ and $8.8 \cdot 10^{-4}$, which means that absolute circular orbits are not possible over time in this system. This is in accordance with the result of Barnes et al. (2009), although one must admit that even the maximum value reached is still very close to a circle, much closer than any planet in our solar system.

Inclination of the system is constant over the whole integration time with a value of 0.0°, therefore movement is restricted to a plane. Maximum difference in eccentricity for the planets is also very low, with a maximum deviation of all planets of $4.3 \cdot 10^{-5}$. The following table gives the maximum and minimum of all massive planets in eccentricity (**e**) and deviations in semi-major axis in AU from initial values (**a**) after the start. Figure 20 gives a graphical display of the integration.

Planet	e min	e max	Δa min	Δa max
b	$2.4 \cdot 10^{-6}$	$7.2 \cdot 10^{-4}$	$-1.3 \cdot 10^{-5}$	$+2.5 \cdot 10^{-6}$
c	$4.1 \cdot 10^{-6}$	$8.8 \cdot 10^{-4}$	$-9.8 \cdot 10^{-6}$	$+1.1 \cdot 10^{-5}$
d	$6.0 \cdot 10^{-7}$	$3.8 \cdot 10^{-4}$	$-1.0 \cdot 10^{-5}$	$+4.3 \cdot 10^{-5}$
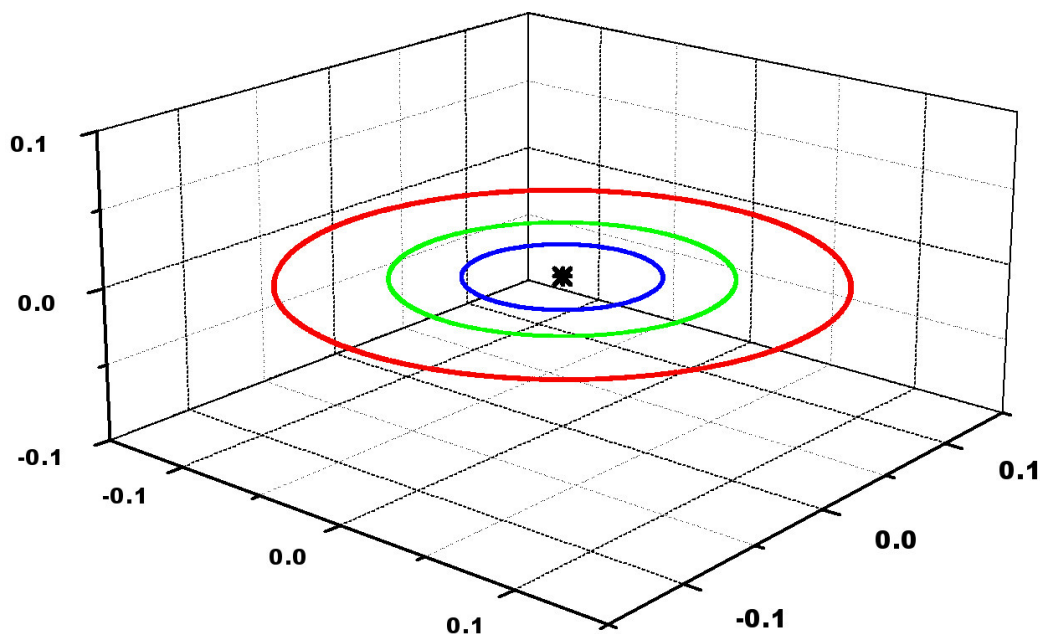
Figure 20: Massive planets of the HD 40307 system, during a 10^6 year integration. Planet b is blue, c is green and d is red. Units are in AU. The central star is indicated by *, and is not scaled.

3.4   HD 40307 - Stability analysis of test bodies

After ensuring the general stability of the massive planets in the system, test planets were again inserted into the system. Since the planets of this system are very close to the central star and the planets are near each other, the system will only be divided into two sections, one including inside all planets and between them, the other one outside all planets. Additionally, mean motion resonances were tested.

The tests themselves were similar to the ones in the HD 60532 system, with most integrated for 10^6 years. Only further out, some test were done for a shorter time. It is noteworthy that in this system, due to the very close semi-major axes of the massive planets, integrations take up much more CPU time than in the system before. This is the main reason why some tests did not include all eccentricities but only three different ones, one with circular orbits, one with average and one with a higher eccentricity, namely an eccentricity of 0.00, 0.05 and 0.10.

Different from the system above, test of this were only performed with an inclination of zero degrees. This is partly due to the planets themselves having no inclination, partly due to the longer CPU time. The other initial conditions are

- a is varied between 0.02 and 10.0 AU, in unregular intervals.

- ω and Ω are always set zero degrees.

Since the three massive planets in this system are situated very close to the central star, the inner and middle section, which were explained separately in the HD 60532 system, are mentioned here together. Generally, all test bodies in this section show a very stable behaviour. The inner most objects were placed at 0.02 AU, which is roughly half way in from the innermost massive planet. This proves to be far enough from the massive planets to be exposed to any major perturbations. For the three tested eccentricities, 0.00, 0.05 and 0.10, the changes in semi-major axes are very close to zero and eccentricity is also almost constant, showing only very slight variation. Inclination is constant at zero degrees for the whole integration period of 10^6 years, meaning that the movement of the test bodies is restricted to the x-y plane in a Cartesian coordinate system. Thus the z component of the massless planets' position vectors is always zero, same as the massive bodies.

Planets are also stable at semi-major axes of 0.03 and 0.04 AU, again for the afore mentioned eccentricities. Tests of planets with average and higher eccentricities at 0.054 AU however proof to lead to instable results, with the planets being ejected in a time between 2000 and 176000 years, higher eccentricities are ejected faster. This behaviour can be explained due to proximity to planet b and to the 4:1 resonance with planet d. At 0.1, only one planet of the four tested is stable, which is the one with the smallest eccentricity of 0.05; at 0.108 AU the two stable planets' e are also below that value.

Curiously, all the integrations of the inner section show one of two behaviours. Either the system is instable, in which case the planet is ejected very fast, within less than 30000 years; the only exception is one planet which lasted for 176000 years. On the other hand, if the planet is stable, the deviations at the end of the integration are very close to zero. Figure 21 gives a graphical representation of two of the before mentioned configurations. The different broadenings due to the different initial eccentricities are clearly visible.
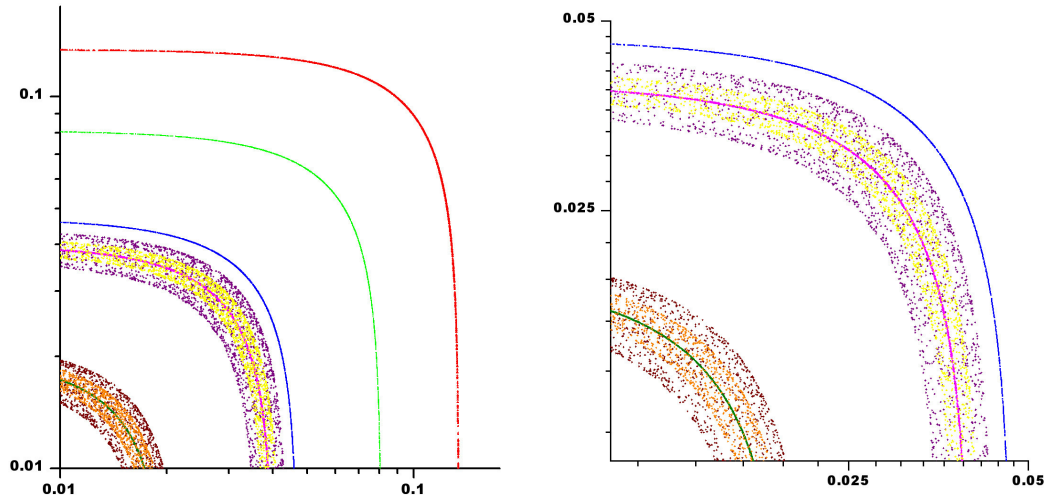
Figure 21: The left graph shows a $\log(x)$ vs $\log(y)$ plot of HD 40307 with two sets of test bodies, at 0.02 and 0.04 AU with an eccentricity of 0.00, given in green and pink, 0.05, in orange and yellow, and 0.1, in wine and purple. The right one zooms on the massless planets. Massive planets are coloured blue, green and red. Units are in AU.

The outer part of this system proves to be even more stable than the inner part. However, the first test bodies at the beginning of this section with a semi-major axis of 0.160 AU are instable. Reasons for this are the higher eccentricities of the objects, reaching from 0.05 to 0.10, as well as the closeness to the massive planet, which is located at 0.134 AU. Interestingly, only two of these planets are ultimately ejected from the system, after 103000 and 377000 years, while the others remain in the system until the end of the integration, which is 1000000 years. They have, however, too much deviation to their initial values to be classified stable, putting them in sticky orbits. Even with such a deviation, all movement of the test particle is still only taking place in the plane drawn by the three massive planets, thus the inclination is still zero degrees. Figure 22 shows the behaviour of one of these test planets moving on a sticky orbit during the integration.
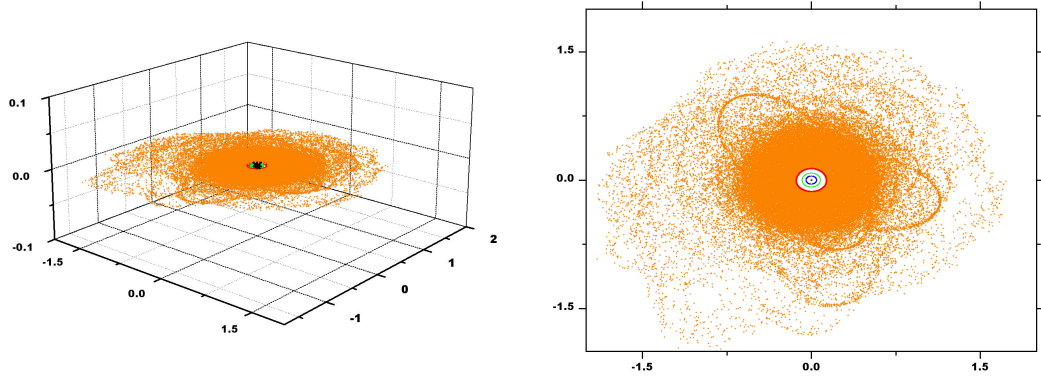
Figure 22: Picture of a test planet with a semi-major axis of 0.16 AU and an eccentricity of 0.08, coloured orange, from the side and top. The massive planets are blue, green and red. Units are in AU.

Top view of the the simulation is given in the right graph in Figure 22, and the central area is given in Fig 23. The paths indicate that some eccentric orbits are run many times by the test planet. In the picture of the central area, the stable orbits at the beginning of the integration are clearly visible, while outwards the area is filled randomly.

Further out, all planets are stable over whole integration time. At 0.17 AU, a test body with an eccentricity of 0.07 has deviations in both eccentricity an semi-major axis almost zero percent. Compared to the maximum changes of the planets, discussed above, the massless body shows stronger perturbations, as expected, with its maximum deviations in semi-major axis in AU being $-2.4 \cdot 10^{-4}$ and $+3.1 \cdot 10^{-4}$, and in eccentricity $-2.8 \cdot 10^{-3}$ and $+3.3 \cdot 10^{-3}$. All these values, although still small, are at least a magnitude higher than the one of the massive planets.

At greater distances to the central star, the deviations decrease. At 0.442 AU, they are about half the amount in semi-major axis and about a magnitude smaller in e than the planet at 0.17 AU. Generally, all the planets present a very stable behaviour, with only slight deviations, as mentioned. Figure 24 shows a typical orbit of such a body. The orbit is closed, as one can see.
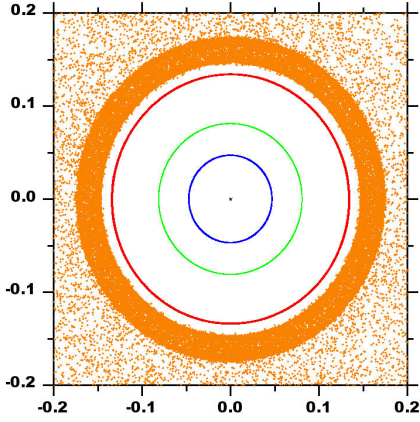
Figure 23: Enhancement of the central section of the right figure in Fig 22.
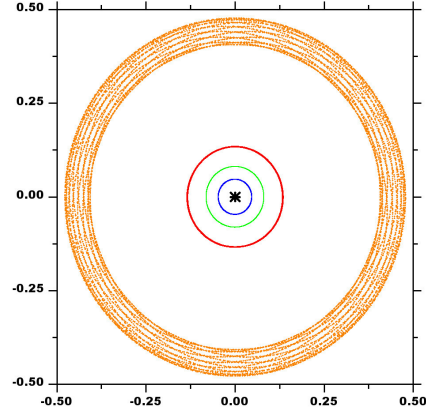
Figure 24: Top view of a test body with an eccentricity of 0.08 at 0.442 AU in orange. Units in AU.

Of certain interest in the study of this system is the behaviour of test planets in mean motion resonances, since stability is given even in between the planets. This is increased even more, since the massive planets themselves are close to a Laplace resonance, even though this is ruled out quite clearly by the discoverers of the planetary system. The massive planets ratio in orbital period according to the information given is $T_b : T_c \simeq 1 : 1.7$ and $T_c : T_d \simeq 1 : 1.7$, which definitely is too far from this special resonance. One of the major questions therefore was, whether massless planets are stable in mean motion resonances, and if yes, if a Laplace resonance is possible between the test bodies and one of the massive planets.

The Laplace resonance has some interesting characteristics. As mentioned before, it is a special configuration, in which the orbital periods of the planets would be in $1 : 2 : 4$ resonances. This was first seen with three of the Galilean satellites of Jupiter, namely Io, Europa and Ganymede. However, no other objects have been found in such a set up.

The $1 : 2 : 4$ resonance imposes certain restrictions on the bodies. Beside the general properties of resonances, with the integer period ratios $p_i : p_{(i+1)}$, which are

$$p_i\lambda_i - p_{(i+1)}\lambda_{(i+1)} + \overline{\omega}_i \quad = \quad const \tag{1}$$

where λ_i is the mean longitude and $\overline{\omega}_i$ the longitude of pericenter, and

$$p_i n_i - p_{(i+1)} n_{(i+1)} + \dot{\overline{\omega}}_i \;\; = \;\; 0 \tag{2}$$

where n_i describes the mean motion; in case of the Galilean satellites

$$
\begin{aligned}
\lambda_I - 2\lambda_E + \overline{\omega}_I &= 0 \\
\lambda_I - 2\lambda_E + \overline{\omega}_E &= \pi \\
\lambda_E - 2\lambda_G + \overline{\omega}_E &= 0
\end{aligned}
\tag{3}
$$

and

$$
\begin{aligned}
n_I - 2n_E + \dot{\overline{\omega}}_I &= 0 \\
n_I - 2n_E + \dot{\overline{\omega}}_E &= 0 \\
n_E - 2n_G + \dot{\overline{\omega}}_E &= 0
\end{aligned}
\tag{4}
$$

there is the Laplace relation

$$
\begin{aligned}
\Phi_L = \lambda_1 - 3\lambda_2 + 2\lambda_3 &= \pi \\
n_1 - 3n_2 + 2n_3 &= 0
\end{aligned}
\tag{5}
$$

Φ_L is the orbital phase. In the case of the Galilean satellites, the resonant argument Φ_L is not fixed to π, but librates around this value. In addition, due to Φ_L, no triple conjunction is possible. Conjunction can happen in the following three situations pictured in Figure 25 (Murray & Dermott 1999 and Ferraz-Mello 1979):

(a) The two inner bodies 1 and 2 are in conjunction. Therefore, $\lambda_3 - \lambda_1 = \frac{\pi}{2}$ (*modulo* π), and consequently the position of body 3 is right-angled to the conjunction line of the other two bodies.

(b) Bodies 1 and 3 are in conjunction. $\lambda_1 - \lambda_2 = \frac{\pi}{3}$ (*modulo* $\frac{2\pi}{3}$). As a result, body 2 is either in opposition to the two other bodies, or at an angle of 60 degrees before or after the two conjugating bodies.

(c) Bodies 2 and 3 are in conjunction, giving $\lambda_1 - \lambda_2 = \pi$ (*modulo* 2π), hence body 1 is in opposition.

36

(a)   (b)   (c)
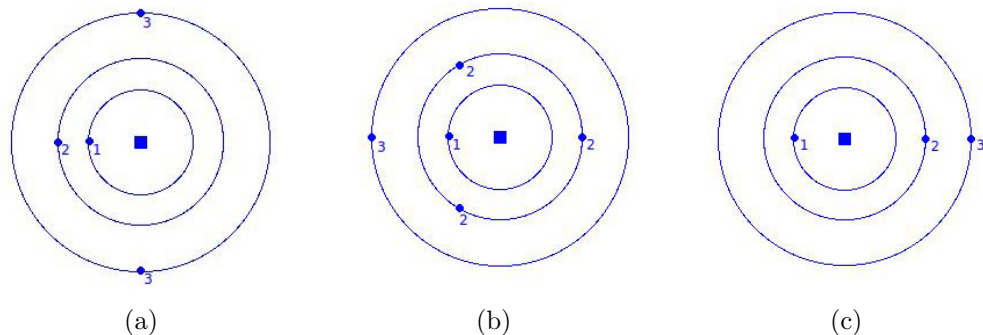
Figure 25: Possibilities of conjunctions in a Laplace resonance. Filled circles are the orbiting bodies, while the filled square is the central object.

The stability of the tested mean motion resonances was first investigated for the most massive of the planets, which is d. The test bodies inserted into the system were placed in a 6:1 to 2:1, in 1:1 resonance in L4, and 1:2 to 1:6 resonance between the test bodies and HD 40307d. All of these resonances were tested with the test bodies having an eccentricity of 0.00 and 0.05. The other outer resonances, including the 1:1 resonance were checked with planets having an eccentricity of 0.10 as well.

The results of the numerical tests done are astonishing. For circular orbits, only two resonances, namely the 2:1 and 5:1 resonance are instable, all other mean resonances are very stable for the whole integration time. For an eccentricity of 0.05, these two, as well as the 4:1 resonance are instable. All other are stable, especially also all outer resonances, even for an eccentricity of 0.10. Most interesting, all three tested eccentricities, 0.00, 0.05 and 0.10, are stable in the 1:1 resonance with planet d. As a result, bodies are possible in planet d's L4.

The instabilities can be explained due to perturbations by planet d, as well as by the closeness to the other two massive bodies, since for the 2:1 resonance, the orbital separation with planet c is only 0.003 AU, for the 5:1 resonance the separation is 0.001 AU. This may also be the reason for the test planet with an eccentricity of 0.05 being instable at the 4:1 resonance, since it again approaches planet b up to a distance of 0.003 AU. Here, it can be seen again that planets are only instable if they move close to one of the massive planets.

Interpreting the results obtained from the tests with respect to a Laplace resonance, one can see that no resonance is possible with planets inside planet d, since the 2:1 resonance is instable. On the other hand, a Laplace resonance is possible between planet d and the test bodies at the 1:2 and 1:4 resonance, which were stable for all tested eccentricities. Since there is also no massive planet further outside, such a configuration, once achieved, could be stable for a long time. Figure 26 shows the behaviour of the stable test bodies with an eccentricity of 0.00 and 0.05 during the integration.
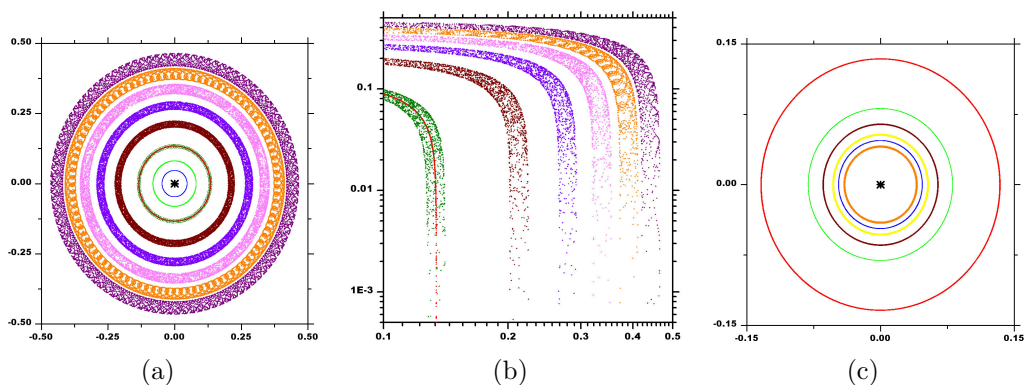
Figure 26: The figure (a) gives the face-on view on the outer mean motion resonances of the test planets with an eccentricity of 0.05. Due to better visibility, in this plot, the points of the 1:1 resonance are smaller than the others'. The graph (b) is a log-log plot of one quadrant of the left one. (c) shows the stable inner resonances of the test planets with an eccentricity of 0.00. Units are in AU, and massive planets are again given by blue, green and red.

Tests have also been performed with the outer resonances of planet c, namely the 1:1 resonance, with the test particle in L4, as well as the 1:2 to 1:4 resonances. Curiously, like with planet d, the 1:1 resonance is stable as well, and so are the 1:3 and 1:4. The deviations in a are almost nil, eccentricity remains almost circular for the whole integration of 10^6 years, as does the inclination, which remains at zero. The 1:2 mean motion resonance proves to be highly instable, with an ejection time of less than 5000 years, which is probably again due to the perturbations of planet d. With the 1:2 resonance instable, no Laplace resonance with the outer resonances is possible for c.
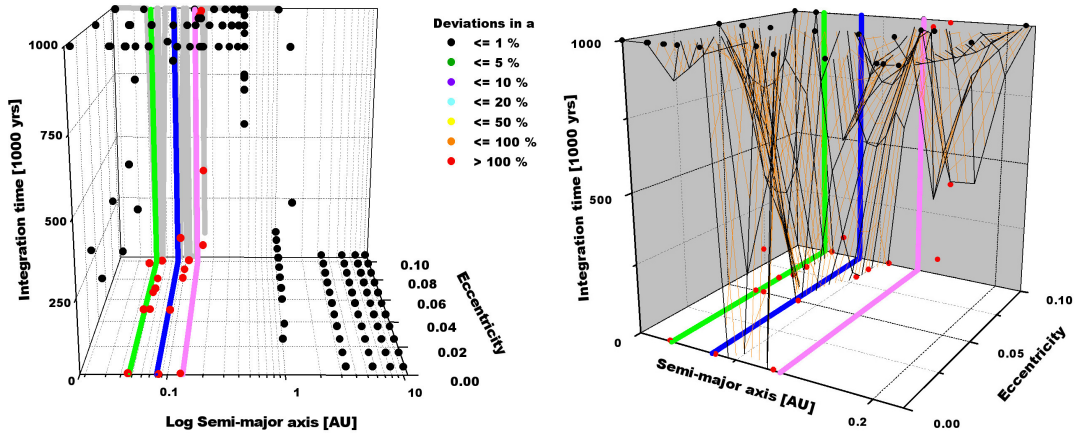
Figure 27: Results of the integrations of the test particles in the HD 40307 system. The massive planets are given by green, blue and pink. The test bodies are coloured according to their stability.

Concluding, this system is very stable, both in random placement as in mean motion resonances. This is pictured in Figures 27 and 28. Note that the outermost planet is now given in magenta instead red for reasons of better distinctions between the planet and instable test particles. Instabilities only arise in the in close proximity to the planets, especially with higher initial eccentricities. Also, some mean motion resonances proved to be instable. Zones of stability and instability are very close, which can especially be seen in the right graph of Fig 27, where the mesh gives the approximate changes between the points. Table 5 gives a comparison of the stability in different regions.
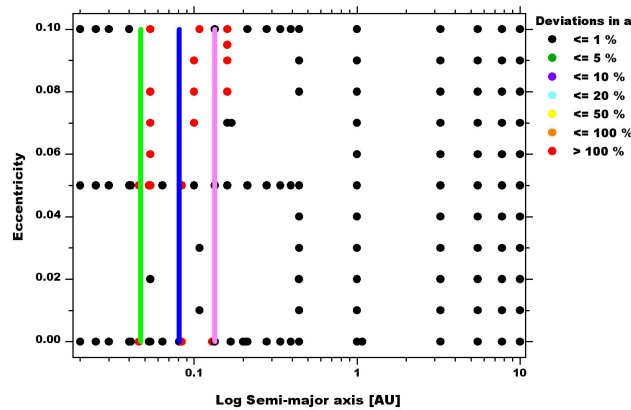
Figure 28: Stability chart.

	Semi-major axis [AU]			
	< 0.042	0.46 - 0.1	0.10 - 0.17	> 0.17
Lower e (0.00 - 0.03)	100	83	80	100
Average e (0.03 - 0.07)	100	22	100	100
Higher e (0.08 - 0.10)	100	0	17	100

Table 5: Overview of how many of the test planets in a configuration are stable, in percent. Higher values mean more stability. The eccentricities are divided into lower and higher values.

4 Secular perturbation

The general N-body problem in celestial mechanics is non integrable, if N is larger than two. However, secular perturbation theory can be used to find analytical solutions for certain problems. First, however, the Lagrange equations and Laplace coefficients must be found. The derivations closely follow Dvorak et al. (2005).

4.1 Lagrange equations

The perturbing function

$$f_i = k^2 \sum_{j=1, j \neq i}^{n} m_j \left(\frac{1}{r_{ij}} - \frac{\vec{q_i} \vec{q_j}}{r_j^3} \right) \tag{6}$$

which is a scalar, can used for the equations of motion of a planet perturbed by others. k^2 denotes the gravitational constant, $\vec{q_k}$ the position vector of the planets and $r_{ij} = |\vec{q_j} - \vec{q_i}|$. f_i can be divided into two parts, one being $\frac{1}{r_{ij}}$, which is the direct part. The indirect part is the inner product of the two $\vec{q_k}$. The direct part of one planet being disturbed by another one is

$$\frac{1}{r_{12}} = \frac{1}{r_2} (1 - 2\zeta \cos \theta + \zeta^2)^{\frac{1}{2}} \tag{7}$$

where θ is the angle between the $\vec{q_k}$, and $\zeta = \frac{r_1}{r_2}$. Additionally, $r_1 < r_2$ is set , and therefore $\zeta < 1$. Thus, an inner planet is perturbed by an outer one. Developing the former equation into a power series and with aid of Legendre polynomials, the perturbing function of a planet with mass m_1 perturbed by a planet with mass m_2 can be written as

$$f_{12} = \frac{k^2 m_2}{r_2} \sum_{n=2}^{\infty} \zeta^n \wp(\cos\theta) \tag{8}$$

$\wp$ stands for the Legendre polynomials. Developing the equation above into a Fourier series in time gives

$$f_{12} = k^2 m_2 \sum_{l=-\infty}^{\infty} \sum_{m=-\infty}^{\infty} A_{lm} \cos((l\ n_1 + m\ n_2)t + B_{lm}) \tag{9}$$

$A_{lm} = A_{lm}(a_1, a_2, e_1, e_2, i_1, i_2)$ are polynomials and can be derived from development into Legendre polynomials. B_{lm} depends on $\omega_1, \omega_2, \Omega_1$ and Ω_2. In a system with more than two planets, perturbation of the other planets on a planet with mass m_1 is the addition of the perturbing functions $f_1 = m_2 f_{12} + \cdots + m_n f_{1n}$. The orbital elements $a_i, e_i, i_i, \Omega_i, \omega_i, M_i$, where M_i is the mean anomaly, influenced by other planets are achieved with a set of first order differential equations. These are the Lagrange equations, and $f = \sum_{m=1}^{n} f_m$.

$$\frac{da}{dt} = \frac{2}{na}\frac{\partial f}{\partial M}$$

$$\frac{de}{dt} = -\frac{\sqrt{1-e^2}}{na^2 e}\frac{\partial f}{\partial \omega} + \frac{1-e^2}{na^2 e}\frac{\partial f}{\partial M}$$

$$\frac{di}{dt} = -\frac{1}{na^2\sqrt{1-e^2}\sin i}\frac{\partial f}{\partial \Omega} + \frac{\cos i}{na^2\sqrt{1-e^2}\sin i}\frac{\partial f}{\partial \omega}$$

$$\frac{d\Omega}{dt} = \frac{1}{na^2\sqrt{1-e^2}\sin i}\frac{\partial f}{\partial i}$$

$$\frac{d\omega}{dt} = \frac{\sqrt{1-e^2}}{na^2 e}\frac{\partial f}{\partial e} - \frac{\cos i}{na^2\sqrt{1-e^2}\sin i}\frac{\partial f}{\partial i}$$

$$\frac{dM}{dt} = n - \frac{2}{na}\frac{\partial f}{\partial a} - \frac{1-e^2}{na^2 e}\frac{\partial f}{\partial e} \tag{10}$$

In addition to the Lagrange equations, knowledge of the Laplace coefficients is needed to derive the secular perturbations.

4.2 Laplace coefficients

The direct part of the perturbing function is given in (7). Expanding this into a Fourier series gives

$$\frac{1}{r_2}(1 - 2\zeta \cos\theta + \zeta^2)^{\frac{1}{2}} = \frac{1}{2}b_{s/2}^{(0)} + \sum_{i=1}^{\infty} b_{s/2}^{(i)} \cos i\theta \qquad (11)$$

s denotes a positive odd integer. The Laplace coefficients $b_{s/2}^{(i)}$ can be calculated by the following formulae

$$\frac{1}{2}(b_{s+1}^{(i)} + b_{s+1}^{(i+1)}) = \frac{(i+s)b_s^{(i)} - (i-s+1)b_s^{(i+1)}}{2s(1-\zeta)^2}$$

$$\frac{1}{2}(b_{s+1}^{(i)} - b_{s+1}^{(i+1)}) = \frac{(i+s)b_s^{(i)} + (i-s+1)b_s^{(i+1)}}{2s(1+\zeta)^2} \qquad (12)$$

For numerical values of the Laplace coefficients see Dvorak et al. (2005).

4.3 Perturbations by two planets

With the Lagrange equations and the Laplace coefficients, it is now possible to derive the secular perturbation theory for two bodies. Once this is done, the perturbations upon a third, massless body can be derived. The derivations are according to the ones given in Murray & Dermott (1999).

Imagine two planets with masses m_1 and m_2 moving around a central mass m_*, with $m_1 << m_*$ and $m_2 << m_*$. f_1 and f_2 are the disturbing functions, which are functions of the osculating orbital elements of both planets, characterising the perturbations on both planets' orbits. The Lagrangian equations (10) specify the perturbations on the orbital elements.

Secular perturbations can be gained by selecting the terms of the disturbing functions that do not depend on the mean longitudes. Hence, the semi-major axis does not contribute, which can be seen in the Lagrange equations. The general, averaged, secular direct part of the disturbing function, after using only terms in second order in eccentricities and inclinantions and first order in masses that do not contain the mean longitude, is

$$\begin{aligned} f_D^{(sec)} = \quad & \frac{1}{8}(2\alpha_{12}D + \alpha_{12}^2 D^2)b_{\frac{1}{2}}^{(0)}(e_1^2 + e_2^2) - \frac{1}{2}\alpha_{12}b_{\frac{3}{2}}^{(1)}(s_1^2 + s_2^2) \\ & + \frac{1}{4}(2 - 2\alpha_{12}D - \alpha_{12}^2 D^2)b_{\frac{1}{2}}^{(1)}e_1 e_2 \cos(\overline{\omega}_1 - \overline{\omega}_2) \\ & + \alpha_{12}b_{\frac{3}{2}}^{(1)}s_1 s_2 \cos(\Omega_1 - \Omega_2) \end{aligned} \qquad (13)$$

whereas $\alpha_{12} = \frac{a_1}{a_2}$, with $a_1 < a_2$, and $s_n = \sin \frac{1}{2}i_n$. Deriving f_1 and f_2 from $f_D^{(sec)}$ gives

$$
\begin{aligned}
f_1 &= \frac{Gm_2}{a_2} f_D^{(sec)} = \frac{Gm_2}{a_1} \alpha_{12} f_D^{(sec)} \\
f_2 &= \frac{Gm_1}{a_2} f_D^{(sec)} = \frac{Gm_1}{a_1} \alpha_{12} f_D^{(sec)}
\end{aligned}
\tag{14}
$$

With help of the following relations of the Laplace coefficients and their derivations

$$
\begin{aligned}
2\alpha \frac{db_{\frac{1}{2}}^{(0)}}{d\alpha} + \alpha^2 \frac{d^2 b_{\frac{1}{2}}^{(0)}}{d\alpha^2} &= \alpha b_{\frac{3}{2}}^{(1)} \\
2b_{\frac{1}{2}}^{(1)} - 2\alpha \frac{db_{\frac{1}{2}}^{(1)}}{d\alpha} - \alpha^2 \frac{d^2 b_{\frac{1}{2}}^{(1)}}{d\alpha^2} &= -\alpha b_{\frac{3}{2}}^{(2)}
\end{aligned}
\tag{15}
$$

and $Gm_* \simeq n_1^2 a_1^3 \simeq n_2^2 a_2^3$ one receives for the perturbation functions

$$
\begin{aligned}
f_1 &= n_1^2 a_1^2 \frac{m_2}{m_* + m_1} \left(\frac{1}{8} \alpha_{12}^2 b_{\frac{3}{2}}^{(1)} e_1^2 - \frac{1}{8} \alpha_{12}^2 b_{\frac{3}{2}}^{(1)} i_1^2 \right. \\
&\quad - \frac{1}{4} \alpha_{12}^2 b_{\frac{3}{2}}^{(1)} e_1 e_2 \cos(\overline{\omega}_1 - \overline{\omega}_2) \\
&\quad \left. + \frac{1}{4} \alpha_{12}^2 b_{\frac{3}{2}}^{(1)} i_1 i_2 \cos(\Omega_1 - \Omega_2) \right) \\
f_2 &= n_2^2 a_2^2 \frac{m_1}{m_* + m_2} \left(\frac{1}{8} \alpha_{12} b_{\frac{3}{2}}^{(1)} e_2^2 - \frac{1}{8} \alpha_{12} b_{\frac{3}{2}}^{(1)} i_2^2 \right. \\
&\quad - \frac{1}{4} \alpha_{12} b_{\frac{3}{2}}^{(1)} e_1 e_2 \cos(\overline{\omega}_1 - \overline{\omega}_2) \\
&\quad \left. + \frac{1}{4} \alpha_{12} b_{\frac{3}{2}}^{(1)} i_1 i_2 \cos(\Omega_1 - \Omega_2) \right)
\end{aligned}
\tag{16}
$$

The assumption in these equations is a small enough i_n so that the approximation $s_n = \sin \frac{1}{2}i_n \simeq \frac{1}{2}i_n$ can be used. Combining equations (16) to

$$
\begin{aligned}
f_j &= n_j a_j^2 \left(\frac{1}{2} A_{jj} e_j^2 + A_{jk} e_1 e_2 \cos(\overline{\omega}_1 - \overline{\omega}_2) \right. \\
&\quad \left. + \frac{1}{2} B_{jj} i_j^2 + B_{jk} i_1 i_2 \cos(\Omega_1 - \Omega_2) \right)
\end{aligned}
\tag{17}
$$

in which $j = 1, 2$; $k = 2, 1$ $(j \neq k)$ and

$$A_{jj} = +n_j \frac{1}{4} \frac{m_k}{m_* + m_j} \alpha_{12} \overline{\alpha}_{12} b_{\frac{3}{2}}^{(1)}(\alpha_{12}) \tag{18}$$

$$A_{jk} = -n_j \frac{1}{4} \frac{m_k}{m_* + m_j} \alpha_{12} \overline{\alpha}_{12} b_{\frac{3}{2}}^{(2)}(\alpha_{12}) \tag{19}$$

$$B_{jj} = +n_j \frac{1}{4} \frac{m_k}{m_* + m_j} \alpha_{12} \overline{\alpha}_{12} b_{\frac{3}{2}}^{(1)}(\alpha_{12}) \tag{20}$$

$$B_{jk} = +n_j \frac{1}{4} \frac{m_k}{m_* + m_j} \alpha_{12} \overline{\alpha}_{12} b_{\frac{3}{2}}^{(1)}(\alpha_{12}) \tag{21}$$

with $\overline{\alpha}_{12} = \alpha_{12}$ if $j = 1$, which is the case in external perturbations and $\overline{\alpha}_{12} = 1$ if $j = 2$, which takes place with internal perturbations. The expressions above can also be written into matrices, in which the elements only depend on the masses and semi-major axes of the two bodies.

$$\mathcal{A} = \begin{pmatrix} A_{11} & A_{12} \\ A_{21} & A_{22} \end{pmatrix} \quad \text{and} \quad \mathcal{B} = \begin{pmatrix} B_{11} & B_{12} \\ B_{21} & B_{22} \end{pmatrix} \tag{22}$$

Using the lowest order terms of e and i in the Lagrange equations one can express the time variation of the elements

$$\dot{e}_j = -\frac{1}{n_j a_j^2 e_j} \frac{\partial f_j}{\partial \overline{\omega}_j} \tag{23}$$

$$\dot{\overline{\omega}}_j = +\frac{1}{n_j a_j^2 e_j} \frac{\partial f_j}{\partial e_j} \tag{24}$$

$$\dot{i}_j = -\frac{1}{n_j a_j^2 i_j} \frac{\partial f_j}{\partial \Omega_j} \tag{25}$$

$$\dot{\Omega}_j = +\frac{1}{n_j a_j^2 i_j} \frac{\partial f_j}{\partial i_j} \tag{26}$$

$$\tag{27}$$

The above equations can become problematic in cases of small i and e. Consequently, new variables are introduced

$$h_j = e_j \sin \overline{\omega}_j \tag{28}$$

$$k_j = e_j \cos \overline{\omega}_j \tag{29}$$

$$p_j = i_j \sin \Omega_j \tag{30}$$

$$q_j = i_j \cos \Omega_j \tag{31}$$

Equation (17) can now be written in the following form

$$
\begin{aligned}
f_j \;=\;\; & n_j a_j^2 (\tfrac{1}{2} A_{jj}(h_j^2 + k_j^2) + A_{jk}(h_j h_k + k_j k_k) \\
& + \tfrac{1}{2} B_{jj}(p_j^2 + q_j^2) + B_{jk}(p_j p_k + q_j q_k))
\end{aligned}
\tag{32}
$$

The perturbation equations can be written in the new variables as

$$
\dot{h}_j \;=\; +\frac{1}{n_j a_j^2}\frac{\partial f_j}{\partial k_j} \tag{33}
$$

$$
\dot{k}_j \;=\; -\frac{1}{n_j a_j^2}\frac{\partial f_j}{\partial h_j} \tag{34}
$$

$$
\dot{p}_j \;=\; +\frac{1}{n_j a_j^2}\frac{\partial f_j}{\partial q_j} \tag{35}
$$

$$
\dot{q}_j \;=\; -\frac{1}{n_j a_j^2}\frac{\partial f_j}{\partial p_j} \tag{36}
$$

$$
\tag{37}
$$

It can be seen in the above equations that, at least for the lowest order, the time derivatives of h_j and k_j are decoupled from the p_j and q_j and vice versa. Since these are linear differential equations with constant coefficients, using the eigenvalues and eigenvectors brings the solutions

$$
h_j \;=\; \sum_{i=1}^{2} e_{ji}\sin(g_i t + \beta_i) \tag{38}
$$

$$
k_j \;=\; \sum_{i=1}^{2} e_{ji}\cos(g_i t + \beta_i) \tag{39}
$$

$$
p_j \;=\; \sum_{i=1}^{2} i_{ji}\sin(f_i t + \gamma_i) \tag{40}
$$

$$
q_j \;=\; \sum_{i=1}^{2} i_{ji}\cos(f_i t + \gamma_i) \tag{41}
$$

The frequencies g_i designate matrix $\mathcal{A}$'s eigenvalues, f_i matrix $\mathcal{B}$'s. Do not mistake the eigenvalue f_i with the disturbing function. e_{ij} and i_{ij} are the elements of the corresponding eigenvectors. β_i and γ_i are phases defined

by the initial conditions. The solutions given by equations (38) to (41) are known as the classical Laplace-Lagrange secular solution.

An interesting feature worth mentioning is that the characteristic equation for $\mathcal{B}$ is

$$\begin{vmatrix} B_{11} - f & B_{12} \\ B_{21} & B_{22} - f \end{vmatrix} = 0 \qquad (42)$$

That can be reduced to

$$f(f - (B_{11} + B_{22})) = 0 \qquad (43)$$

and means that one solution is $f = 0$, which gives a degeneracy problem. This is a difference between h, k variables, which involve eccentricity, and p, q, which involve inclination. An eccentric orbit provides an asymmetry and thus a reference line, a point-mass body gives no natural reference plane. Consequently, only mutual inclinations are meaningful.

Also, the solution given above is not depending upon the mean longitude. As a result, only variations in eccentricities, inclinations, pericenters and nodes are predictable, not the actual positions of the planets themselves.

4.4 The HD 60532 configuration

Following the steps given above, the perturbations of both massive planets of the HD 60532 system can be investigated. For this purpose, the inclination and longitude of the ascending node of both planets were changed to be slightly unequal, namely one degree difference in i and ten degrees in Ω. The reference plane of the inclination was changed as well, such that the inner planet has an inclination with respect to the new plane of 1.5°, while the outer one's is 2.5°. The calculation was performed with the program Wolfram Mathematica.

In this configuration, $\alpha_{12} = \frac{a_1}{a_2} = 0.48734$, thus the values for the Laplace coefficients are

$$b_{\frac{3}{2}}^{(1)} = 2.43759$$

$$b_{\frac{3}{2}}^{(2)} = 1.43722 \qquad (44)$$

The calculation of the Laplace coefficients was done with Mathematica packages provided by F. Zugno (2002). The matrix elements of the disturbing functions then have the following values

$$\mathcal{A} = \left(\begin{array}{cc} +0.380633 & -0.224423 \\ -0.0659659 & +0.111881 \end{array} \right)$$

and

$$\mathcal{B} = \left(\begin{array}{cc} -0.380633 & +0.380633 \\ +0.111881 & -0.111881 \end{array} \right)$$

Solving the characteristic equations gives the eigenvalues of $\mathcal{A}$ and $\mathcal{B}$.

$$\begin{array}{rcl} g_1 & = & +0.0649807° \ yr^{-1} \\ g_2 & = & +0.427533° \ yr^{-1} \\ f_1 & = & +0.0° \ yr^{-1} \\ f_2 & = & -0.492514° \ yr^{-1} \end{array} \qquad (45)$$

The next step is to calculate the eigenvectors of both matrices. However, each eigenvector is determined only up to a scaling constant. Therefore, the normalised eigenvectors are

$$\begin{array}{rcl} \vec{\varepsilon_1} & = & \left(\begin{array}{c} +0.579455 \\ +0.815005 \end{array} \right) \\ \vec{\varepsilon_2} & = & \left(\begin{array}{c} +0.978853 \\ -0.204564 \end{array} \right) \\ \vec{\iota_1} & = & \left(\begin{array}{c} -0.707107 \\ -0.707107 \end{array} \right) \\ \vec{\iota_2} & = & \left(\begin{array}{c} -0.959413 \\ 0.282005 \end{array} \right) \end{array} \qquad (46)$$

The scaling constant can be found with the boundary conditions. Setting t=0 for equations of the new variables, (28) to (31), as well as for the solutions of these, (38) and (41), one receives four sets of simultaneous linear equations. These are used to determine the unknown numbers. Denoting that X_i is the scaling factor of $\vec{\varepsilon_i}$ and Y_i of $\vec{\iota_i}$ one receives

$$X_1 = 0.049912 \quad \text{and} \quad X_2 = 0.262323$$
$$Y_1 = 0.055991 \quad \text{and} \quad Y_2 = 0.014839 \tag{47}$$

The phase angles given in the solutions are determined to be the following values

$$\beta_1 = -29.5° \quad \text{and} \quad \beta_2 = 15.5°$$
$$\gamma_1 = 151.5° \quad \text{and} \quad \gamma_2 = -44.3° \tag{48}$$

The corrected eigenvectors are thus

$$\vec{e}_1 = \begin{pmatrix} +0.028922 \\ +0.040679 \end{pmatrix}$$
$$\vec{e}_2 = \begin{pmatrix} +0.256776 \\ -0.053662 \end{pmatrix}$$
$$\vec{i}_1 = \begin{pmatrix} -0.039592 \\ -0.039592 \end{pmatrix}$$
$$\vec{i}_2 = \begin{pmatrix} -0.014236 \\ +0.004185 \end{pmatrix} \tag{49}$$

The $\vec{i}_j$ are given in degrees. With all the values now determined, $e_j(t)$, $\overline{\omega}_j(t)$, $i_j(t)$ and $\Omega_j(t)$, with $j = 1, 2$ for the two planets, can now be calculated by

$$e_j(t) = \sqrt{h_j^2 + k_j^2}$$
$$\overline{\omega}_j(t) = \arccos \frac{k_j}{e_j}$$
$$i_j(t) = \sqrt{p_j^2 + q_j^2}$$
$$\Omega_j(t) = \arccos \frac{q_j}{i_j} \tag{50}$$

In case of rotating angles, one must take care of the switches between the arccos branches. Using the cosine rule for e and i, one finally receives

$$e_j(t) = \sqrt{e_{j1}^2 + e_{j2}^2 + 2e_{j1}e_{j2}\cos((g_1 - g_2)\cdot t + \beta_1 - \beta_2)}$$
$$i_j(t) = \sqrt{i_{j1}^2 + i_{j2}^2 + 2i_{j1}i_{j2}\cos((f_1 - f2)\cdot t + \gamma_1 - \gamma_2)} \tag{51}$$

or, inserting digits

$$
\begin{aligned}
e_1(t) &= \sqrt{0.06677 + 0.0148528 \cdot \cos(0.362553 \cdot t + 44.9391°)} \\
e_2(t) &= \sqrt{0.00453 - 0.0043658 \cdot \cos(0.362553 \cdot t + 44.9391°)} \\
i_1(t) &= \sqrt{0.00177 + 0.0011273 \cdot \cos(0.492514 \cdot t + 195.782°)} \\
i_1(t) &= \sqrt{0.00159 - 0.0003313 \cdot \cos(0.492514 \cdot t + 195.782°)}
\end{aligned}
\tag{52}
$$

As one can see, the frequency of the planets are rather short, with both having an period in eccentricity of about 1000 years and about 750 years in inclination. Figure 29 shows the interactions in eccentricity between the two planets. The inner planet has the colour blue, while the outer one is green. Note that an outer planets maxima of eccentricity is aligned with the inner's minima and vice versa. Remember that a mean motion resonance exists as well between the planets, introducing additional perturbations on a shorter timescale, which are not accounted for in secular resonances.
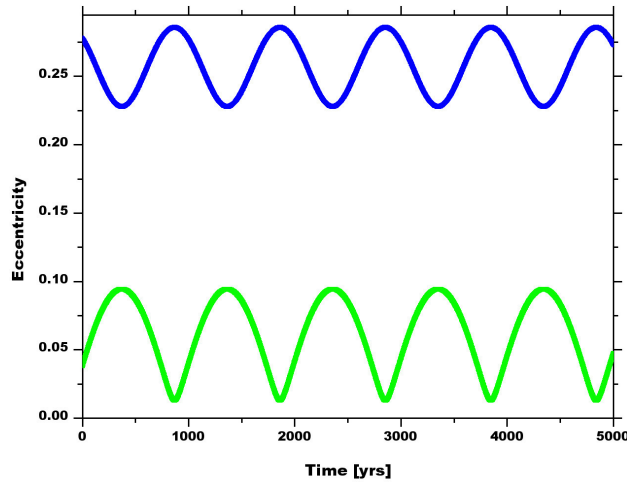
Figure 29: Secular perturbations in eccentricity between the two massive bodies in HD 60532. Planet b is coloured blue, while c is green. For explanations see text.

Figure 30 gives a comparison between the results of the secular perturbation approach and a numerical integration. Note that the integration displays a longer time. Interestingly, planet c's changes given by secular perturbations are reduced little, while planet b experiences additional excitement. Additionally, the lower boundary of both coincides with the secular solution.
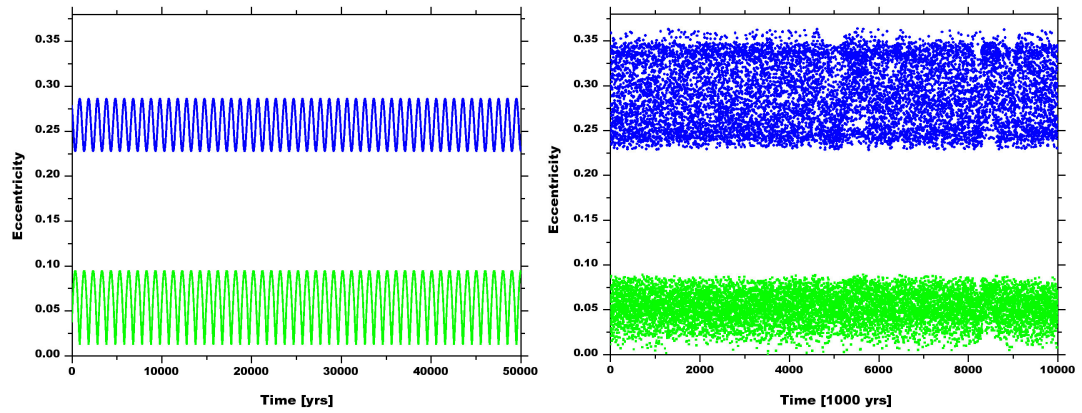
Figure 30: The left picture shows the secular perturbations in eccentricity between the two bodies for a time of 50000 years. The right is shows a numerical integration of the two bodies.

Figure 31 shows the perturbations in inclination. Again, the minima of one planet correlates with the maxima of the other. Note also the good accordance between numerical and analytical solutions in Fig 32.
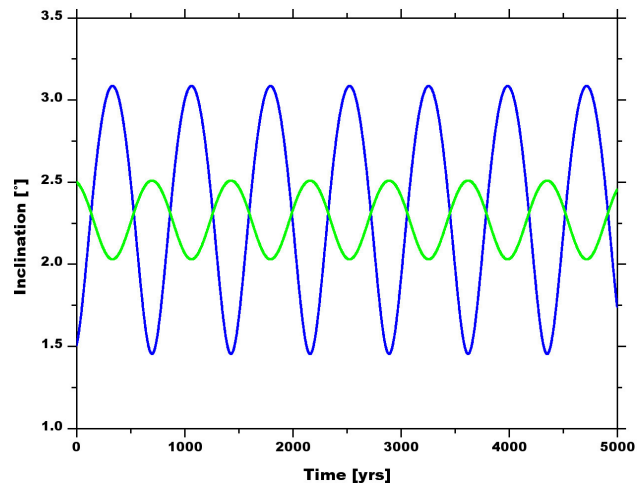
Figure 31: Secular perturbations in inclination between the two bodies.

50
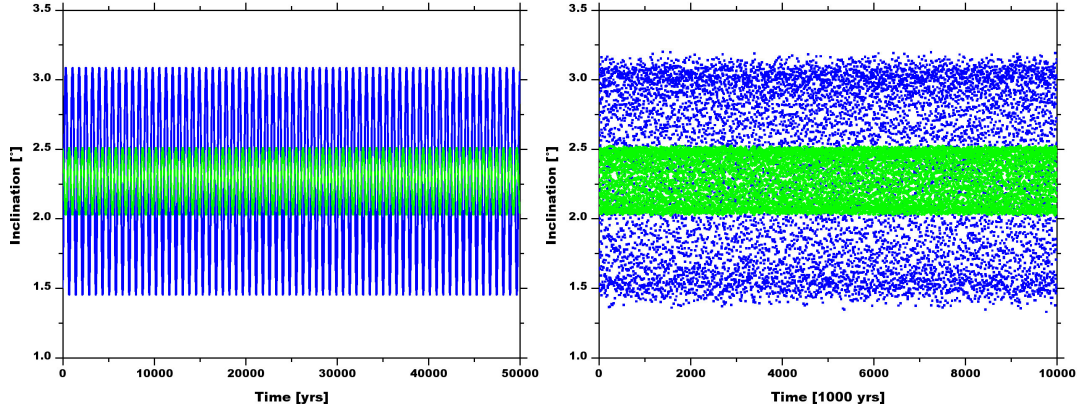
Figure 32: The left picture shows the secular perturbations in inclination between the two bodies for a time of 50000 years. The right is shows the results in inclination of a numerical integration of the two bodies.
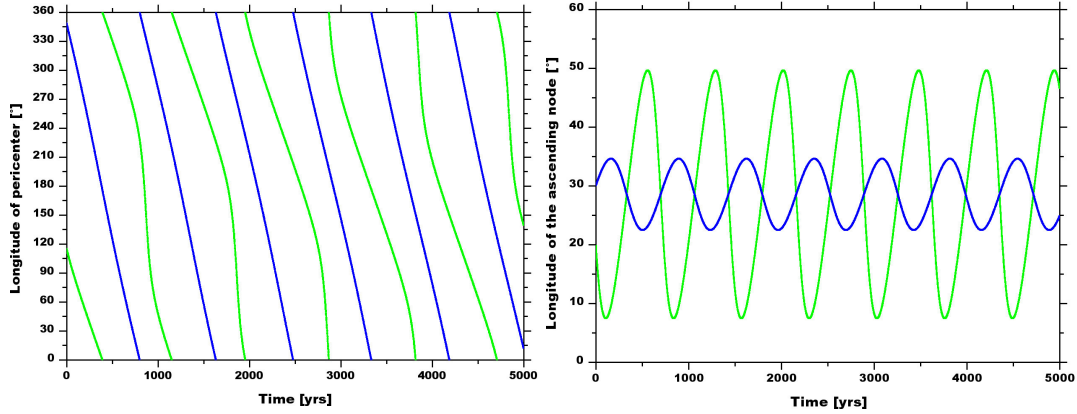
Figure 33: The left picture shows the secular perturbations in $\overline{\omega}$. The right in Ω.

The changes of $\overline{\omega}$ and Ω are given in Fig 33. The former rotates like in the integrations. Note that planet c shows changes in $\overline{\omega}$, while b does not. The latter, like i, is presented very well again with secular perturbation effects, with integrations having the inner planet oscillating between 4 and 51°, while the outer one is in the range between 23 to 35°.

4.5   Inserting a massless body

The equations above can now be used to see the perturbations upon a third, massless body. The disturbing function for a test object with the orbital elements a, e, i, $\overline{\omega}$, Ω and n is

$$
\begin{aligned}
f \;=\; & na^2\Big(\tfrac{1}{2}Ae^2 + \tfrac{1}{2}Bi^2 + \sum_{j=1}^{2} A_j ee_j \cos(\overline{\omega} - \overline{\omega}_j) + \\
& + \sum_{j=1}^{2} B_j ii_j \cos(\Omega - \Omega_j)\Big)
\end{aligned}
\tag{53}
$$

in which

$$
A \;=\; +n\frac{1}{4}\sum_{j=1}^{2}\frac{m_j}{m_*}\alpha_j\overline{\alpha}_j b_{\frac{3}{2}}^{(1)}(\alpha_j)
\tag{54}
$$

$$
A_j \;=\; -n\frac{1}{4}\frac{m_j}{m_*}\alpha_j\overline{\alpha}_j b_{\frac{3}{2}}^{(2)}(\alpha_j)
\tag{55}
$$

$$
B \;=\; -n\frac{1}{4}\sum_{j=1}^{2}\frac{m_j}{m_*}\alpha_j\overline{\alpha}_j b_{\frac{3}{2}}^{(1)}(\alpha_j)
\tag{56}
$$

$$
B_j \;=\; +n\frac{1}{4}\frac{m_j}{m_*}\alpha_j\overline{\alpha}_j b_{\frac{3}{2}}^{(1)}(\alpha_j)
\tag{57}
$$

and

$$
\begin{aligned}
\alpha_j &= \begin{cases} \frac{a_j}{a} & if \quad a_j < a \\ \frac{a}{a_j} & if \quad a_j > a \end{cases} \\
\overline{\alpha}_j &= \begin{cases} 1 & if \quad a_j < a \\ \frac{a}{a_j} & if \quad a_j > a \end{cases}
\end{aligned}
\tag{58}
$$

The new variables for the massless body are

$$
\begin{aligned}
h &= e\sin\overline{\omega} \tag{59}\\
k &= e\cos\overline{\omega} \tag{60}\\
p &= i\sin\Omega \tag{61}\\
q &= i\cos\Omega \tag{62}
\end{aligned}
$$

The variables of the massive bodies perturbing the test object, denoted h_j, k_j, p_j and q_j are given in (28) to (31). The disturbing function in new variables is

$$
\begin{aligned}
f \;=\; & na^2\left(\frac{1}{2}A(h^2 + k^2) + \frac{1}{2}B(p^2 + q^2)\right. \\
& \left. + \sum_{j=1}^{2} A_j(hh_j + kk_j) + \sum_{j=1}^{2} B_j(pp_j + qq_j)\right)
\end{aligned}
\tag{63}
$$

leading to the following equations of motion

$$
\dot{h} \;=\; +\frac{1}{na^2}\frac{\partial f}{\partial k}
\tag{64}
$$

$$
\dot{k} \;=\; -\frac{1}{na^2}\frac{\partial f}{\partial h}
\tag{65}
$$

$$
\dot{p} \;=\; +\frac{1}{na^2}\frac{\partial f}{\partial q}
\tag{66}
$$

$$
\dot{q} \;=\; -\frac{1}{na^2}\frac{\partial f}{\partial p}
\tag{67}
$$

By inserting equation (63) in equations (64) to (67), one can rewrite the equations of motion to

$$
\dot{h} \;=\; +Ak + \sum_{j=1}^{2} A_j k_j
\tag{68}
$$

$$
\dot{k} \;=\; -Ah - \sum_{j=1}^{2} A_j h_j
\tag{69}
$$

$$
\dot{p} \;=\; +Bq + \sum_{j=1}^{2} B_j q_j
\tag{70}
$$

$$
\dot{q} \;=\; -Bp - \sum_{j=1}^{2} B_j p_j
\tag{71}
$$

Using the h_j, k_j, p_j and q_j from equations (38) to (41) gives

$$\dot{h} \;\; = \;\; +Ak + \sum_{j=1}^{2} A_j \sum_{i=1}^{2} e_{ji} \cos(g_i t + \beta_i) \tag{72}$$

$$\dot{k} \;\; = \;\; -Ah - \sum_{j=1}^{2} A_j \sum_{i=1}^{2} e_{ji} \sin(g_i t + \beta_i) \tag{73}$$

$$\dot{p} \;\; = \;\; +Bq + \sum_{j=1}^{2} B_j \sum_{i=1}^{2} i_{ji} \cos(f_i t + \gamma_i) \tag{74}$$

$$\dot{q} \;\; = \;\; -Bp - \sum_{j=1}^{2} B_j \sum_{i=1}^{2} i_{ji} \sin(f_i t + \gamma_i) \tag{75}$$

By differentiating these equations one more time with respect to the time one obtains

$$\ddot{h} \;\; = \;\; -A^2 h - \sum_{j=1}^{2} \eta_i (A + g_i) \sin(g_i t + \beta_i) \tag{76}$$

$$\ddot{k} \;\; = \;\; -A^2 k - \sum_{j=1}^{2} \eta_i (A + g_i) \cos(g_i t + \beta_i) \tag{77}$$

$$\ddot{p} \;\; = \;\; -B^2 p - \sum_{j=1}^{2} \varsigma_i (B + f_i) \sin(f_i t + \gamma_i) \tag{78}$$

$$\ddot{q} \;\; = \;\; -B^2 q - \sum_{j=1}^{2} \varsigma_i (B + f_i) \cos(f_i t + \gamma_i) \tag{79}$$

using

$$\eta_i \;\; = \;\; \sum_{j=1}^{2} A_j e_{ji}$$

$$\varsigma_i \;\; = \;\; \sum_{j=1}^{2} B_j i_{ji} \tag{80}$$

One can see that equations (76) to (79) are a system of uncoupled differential equations with the solutions

$$h = e_{free}\sin(At + \beta) + h_0(t) \tag{81}$$
$$k = e_{free}\cos(At + \beta) + k_0(t) \tag{82}$$
$$p = i_{free}\sin(Bt + \gamma) + p_0(t) \tag{83}$$
$$q = i_{free}\cos(Bt + \gamma) + q_0(t) \tag{84}$$

The constants e_{free}, i_{free}, β and γ are determined from the boundary conditions, and

$$h_0(t) = -\sum_{i=1}^{2} \frac{\eta_i}{A - g_i}\sin(g_i t + \beta_i) \tag{85}$$

$$k_0(t) = -\sum_{i=1}^{2} \frac{\eta_i}{A - g_i}\cos(g_i t + \beta_i) \tag{86}$$

$$p_0(t) = -\sum_{i=1}^{2} \frac{\varsigma_i}{B - f_i}\sin(f_i t + \gamma_i) \tag{87}$$

$$q_0(t) = -\sum_{i=1}^{2} \frac{\varsigma_i}{B - f_i}\cos(f_i t + \gamma_i) \tag{88}$$

These functions only depend on the semi-major axes of the test objects, which are constant, but they do vary with time, since there is a dependence upon the secular solution of the perturbators. Thus, the elements of the massless bodies are a combination of both the initial elements of the massless object, as well as the forced ones by the massive bodies.

The forced amounts on the particles orbital elements are given by

$$e_{forced} = \sqrt{h_0^2 + k_0^2}$$
$$i_{forced} = \sqrt{p_0^2 + q_0^2}$$
$$\overline{\omega}_{forced} = \arccos\left(\frac{k_0}{e_{forced}}\right)$$
$$\Omega_{forced} = \arccos\left(\frac{q_0}{i_{forced}}\right)$$

$$\tag{89}$$

4.6   Massless body in HD 60532

In order to calculate the perturbations on a massless test body in the HD 60532 system, the first thing to do is to calculate the elements of the disturbing function A, A_j, B and B_j. Note that, as used in this case, $B = -A$ for a point source central object. These are all functions of the the massive planets' mass, and α_j, the ratio of the planets' and test particle's semi-major axis. Figure 34 gives a graphical representation of A. The singularity arises from the Laplace coefficients, which go to infinity as α_j approaches one. Also, since both planets are very close together, both overlap and create only one singularity, with both peaks only separated for values of $2.3°\ yr^{-1}$ or higher.
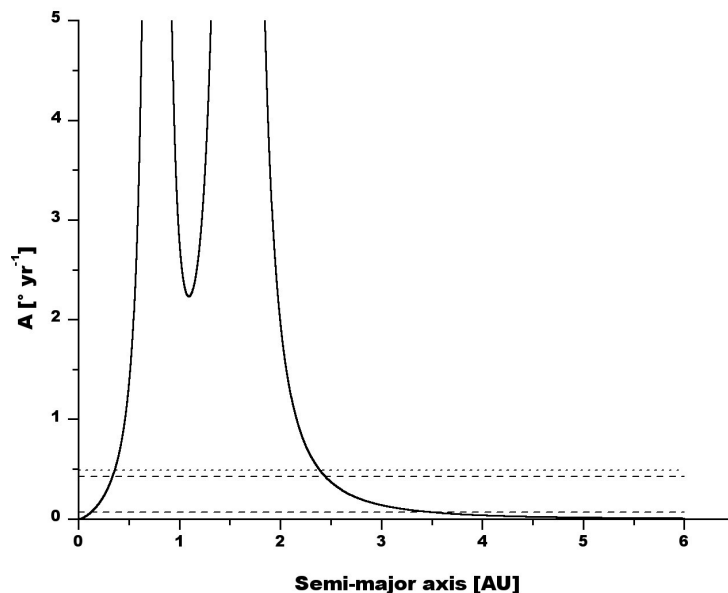
Figure 34: Behaviour of the element A of the disturbing function. The dashed lines denote the two eigenvalues of matrix $\mathcal{A}$, while the doted represents matrix $\mathcal{B}$'s.

Having achieved this, these elements are inserted into equations (85) to (88). Problems will also arise in these equations, when the values of A and B reach these of the eigenvalues, since the denominator tends to zero, given by the intersection between the graph and the doted and dashed lines in Fig 34. The eigenvalues were already calculated in section 4.4, and are namely $g_1 = 0.065°\ yr^{-1}$ and $g_2 = 0.428°\ yr^{-1}$, as well as $f2 = -0.493°\ yr^{-1}$. Therefore, since there are two non zero eigenvalues, four singularities are expected for e and ω; two for i and Ω.

56

The following figures give a graphical overview of the forced changes of the test particles. These give changes to the test particles orbital elements due to secular perturbations. Remember that there are changes with time, therefore the figures give a representation at $t = 0$.
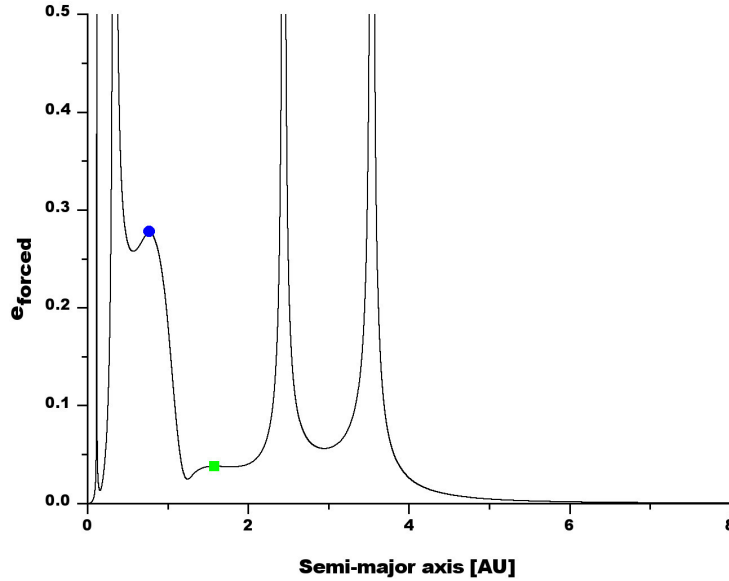
Figure 35: Forced eccentricity of massless bodies in the HD 60532 system. The massive planets are given in blue and green.

The four singularities of forced eccentricity are located at 0.117, 0.34, 2.4 and 3.5 AU. The latter three peaks, especially the first of these, have a rather wide extension, thus adding to the destabilisation of the inner part of the system. The second and third also account for the instabilities in the outer section of the system, with the first stable planets appearing only outside of both. The first singularity however lies in the already stable section inside 0.2 AU. It is on the other hand restricted to a small area, with forced eccentricities above 0.1 only in the section between 0.11 and 0.12 AU. Also, even with a high eccentricity, objects in this region would still lie below the 0.2 AU boundary, and sustainability could still be possible for most particles. The forced eccentricity reaches values near zero at 5 AU.

The singularities appear at the same locations for $\overline{\omega}$. Most distances show excitement between 80 and 120°. Since both massive planets rotate with time, also the massless planets are rotating, as can be seen in integrations. The graph below shows the situation at the initial condition.
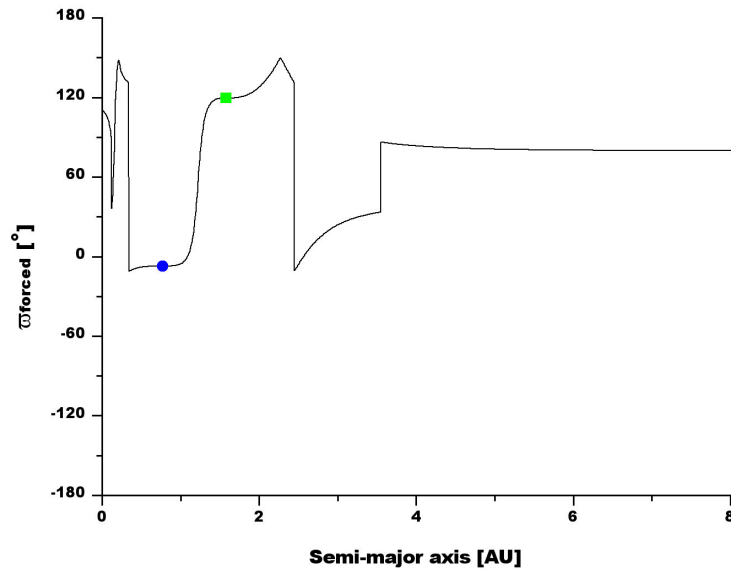
Figure 36: Forced longitude of the perihelion of massless bodies in the HD 60532 system.

For i of the massless bodies, the inclinations as above were used, namely 1.5 and 2.5°, since if no difference is set between the two massive bodies, also none arises for the massless. Like mentioned above, there are only two singularities, which are also confined to a small area. The general forced inclination is situated at about 2.2° for the massless bodies.
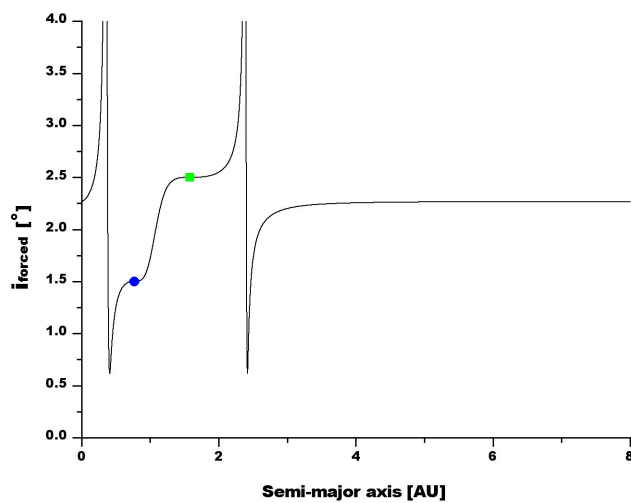
Figure 37: Forced inclination of massless bodies in the HD 60532 system.

Again, the singularities of Ω are located at the same place as i's, which is located in the instable zone as investigated in the n-body integrations. The forced longitude of the ascending node is at 28° in the stable zones.
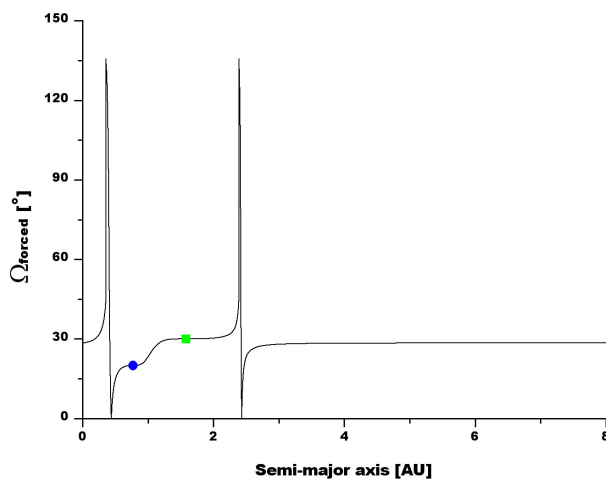
Figure 38: Forced longitude of the ascending node of massless bodies in the HD 60532 system.

5 Conclusion

This thesis investigates the stability of possible Earth-mass planets in two extrasolar systems where two and three planets respectively had already been found. Methods used were both n-body integration, as well as secular perturbation theory. The systems involved were HD 60532 and HD 40307. Both systems were discovered in 2008, and have massive bodies close to the central star, in case of the former Jupiter-sized, while in the latter mini Neptunes or super Earths. Integration was performed with a Lie integrator.

Results of the integrations performed during this thesis showed that the HD 60532 planetary system, harboring two planets with 3.15 and 7.46 Jupiter masses, is stable for a long time, with the longest integration lasting for more than 65 million years, although strong interactions happen between the two planets. Changing the inclination of both planets away from coplanar orbits to slight inclinations towards each other can reduce these interactions. Generally, both planets' argument of the perihelion ω rotates, while the longitude of the ascending node Ω librates in most cases, however, rotation also happened in some cases. With a different starting inclination i, the outcome is either that planet c's i is the average of planet b's, or that the more massive planet c is having a low i compared to b, which is excited. The most stable solution was found with planet b having an inclination of 1.5° and longitude of the ascending node of 20°, while planet c's inclination was 2.5° and Ω 30°. Due to the eccentricity especially of the inner planet, a large section between the two planets is covered by the orbits of both planets. This has a negative effect on the stability of the massless bodies inserted.

Instability for test bodies in this system located during the integrations indeed extended over a large section, between 0.2 and 3.6 AU, where particles are perturbed heavily by the massive planets. Inside respectively outside these borders, stability is possible and increasing with distance to the massive planets. Tests were performed with different initial inclinations of test bodies, namely zero, five, 15 and 20 degrees with respect to the plane of the massive planets, but these variations only showed little effects. Stability for all test particles, which were inserted within an range of 0.0 to 0.1 with steps of 0.01 in eccentricity, was reached at 5.0 to 6.0 AU. On the inside, all particles were stable at semi-major axes of 0.123 AU. Between these distances and the instable zone, some planets are stable, while others are not. There is no certain trend depending on the eccentricity e of the massless planets on the inside, on the outside stable planets mainly have a low or average e.

Tests on mean motion resonances were done for zero and 20° inclination configurations, though results normally were only stable if placed in an already stable region. Also, 1:1 resonance in both Lagrangian points L4 and L5 proved to be instable.

As second part done in this thesis, secular resonance investigations of the system revealed a period of about 1000 years in the variations of eccentricity and 750 years for the inclination. Both planets show opposite movement, i.e. a maxima of planet b occurs at c's minima and vice versa. These resonances only make up for a part of the integrations changes of eccentricity, since the massive planets' 3:1 mean motion resonances are not accounted, which acts on a shorter timescale. However, the inner border of both planets' eccentricity in the n-body integrations coincides with the secular's. Inclination and longitude of the ascending nodes are represented well by secular perturbations, and the longitude of perihelion rotates as it does in integrations, with c's altering in speed.

Inserting massless bodies into the configuration with secular theory shows that there exists a space of instability inside the inner boundary of stability given by the integrations, at 0.117 AU. However, it is confined to a small space. Between the bodies and only little outside planet c, stable zones would exist, however other effects give rise to instabilities, since none was found with integrations. In the other stable zones given by the integrations, forced eccentricity is down to almost zero. Forced inclination rises the bodies to almost the values of planet c, as does forced longitude of the ascending node and of perihelion. In the latter however, since the massive planets rotate, this incitation only plays a subordinate role over a long time scale.

The HD 40307 system harbors three planets with masses between 0.0132 and 0.0288 Jupiter masses, in orbits very close to the central star. Integrations performed of the massive planets showed stability is given, with deviations in orbital elements being almost nil. However, orbits of the planets do not remain circular but become very slightly elliptic. Since the other orbital elements are the same, no changes occur, especially since all planets move on the same plane.

The bodies inserted in the tests were placed between 0.02 and 10.0 AU, and eccentricities were specified zero, 0.05 and 0.10 in most cases, although also others were chosen. The stability in this system is given for most configurations, with limits only applying to test particles close to the given planets, especially with higher initial eccentricities, again leading to close encounters.

Certain mean motion resonances however are instable, even with an e of 0.0. Simulations showed that bodies are stable in most mean motion resonances, even with an eccentricity of 0.05, or, where tested, 0.10. Particles placed into Lagrangian points L4 of two of the massive planets remain on regular orbits, for planet d even with eccentricities of up to 0.10. Also, a Laplace resonance is possible in this system between planet d and bodies in outer mean motion resonances, though not the same applies for planet c. If planets are stable, the deviations in semi-major axis and eccentricity remain close to zero. This concludes the research done during this thesis. Study of the stability of multiplanetary systems will however continue to be an important part of astrophysics, since the formation of more than one planet is very likely in most cases.

6   Zusammenfassung

Ziel dieser Magisterarbeit ist die Untersuchung der Stabilität von möglichen Planeten mit Erdmassen in zwei extrasolaren Systemen, in denen bereits zwei bzw. drei Planeten entdeckt wurden. Die verwendeten Methoden sind n-Körper Integrationen sowie säkulare Störungstheorie. Die betrachteten Systeme sind HD 60532 und HD 40307, beide wurden im Jahr 2008 entdeckt und haben massereiche Körper nahe dem Zentralstern, im Falle des ersten in Jupitergrößenordnung, im letzteren Mini-Neptun oder Super-Erden. Die Integration wurde mit einem Lie-Integratior durchgeführt.

Die Resultate der hier betriebenen Integrationen zeigten, dass HD 60532, mit zwei Planeten von 3.15 und 7.46 Jupitermassen, über lange Zeiträume stabil ist, obwohl starke Wechselwirkungen zwischen den Planeten auftreten. Die längste Integration dauerte 65 Millionen Jahre. Werden die Inklinationen beider Planeten nicht als koplanar angenommen, sondern leicht zueinander verändert, kann eine Abschwächung der Wechselwirkungen auftreten. Im Allgemeinen rotiert das Argument des Periapsis ω beider Planeten, während das Argument des Knotens Ω in den meisten Fällen libriert. Es gibt jedoch auch Fälle, in denen eine Rotation stattfindet. Das Ergebnis bei zueinander verschiedenen Startinklinationen ist entweder, dass die Inklination i von c den Mittelwert von b bestimmt, oder dass der massivere c ein kleines i hat, während b angeregt wird. Die stabilste Konfiguration war eine Inklination von 1.5° und ein Ω von 20° für b und 2.5° Inklination und ein Ω von 30° für c. Ein großer Teil der Raumes zwischen den Planeten wird von den Orbits beider Planeten abgedeckt, was sich negativ auf die Stabilität von Probekörpern auswirkt.

Die in den Integrationen gefundenen Instabilitäten dieses Systems breiten sich weiträumig aus, nämlich zwischen 0.2 und 3.6 AE. Hier werden die Testkörper stark von den massiven Planeten gestört. Innerhalb und ausserhalb dieser Grenzen ist jedoch Stabilität möglich und steigt mit zunehmenden Abstand. Unterschiedliche Startwerte der Inklination der Probekörper, genauer gesagt null, fünf, 15 und 20 Grad in Bezug auf die Bahnebene der Planeten, ändern die Ergebnisse nur geringfügig. Stabilität aller Testkörper, welche mit Exzentrizitäten von 0.0 bis 0.1 und einer Schrittweite von 0.01 eingefügt wurden, ergibt sich bei einer großen Halbachse a von 5.0 bis 6.0 AE auf der Außenseite, und 0.123 AE auf der Innenseite.

Zwischen diesem Bereich und der instabilen Zone wird für manche Körper Stabilität erreicht, für andere hingegen nicht. Auf der Innenseite ist kein von der Exzentrizität e abhängiger Trend erkennbar, während auf der Außenseite stabile Planeten eher kleine bis mittlere e haben. Für die Konfigurationen mit Inklinationen von null und 20° wurden auch Bahnresonanzen getestet, wobei herausgefunden wurde, dass diese normalerweise nur dann stabil sind, wenn sie bereits in einer stabilen Region liegen. Auch die 1:1 Resonanz, mit Testkörpern in den Lagrangepunkten L4 und L5, ist instabil.

Als zweiter Teil dieser Arbeit wurden die säkularen Störungseffekte im System berechnet, was als Ergebnis eine Variation der e beider Planeten mit einer Periode von 1000 Jahren ergab, in i von 750 Jahren, wobei das Maximum eines Planeten mit dem Minimum des anderen zusammenfällt. Diese Resonanz macht jedoch nur einen Teil der in der Integration gefundenen Änderungen aus, da die bestehende 3:1-Resonanz zwischen den Planeten nicht einbezugen ist, welche auf kürzeren Zeiträumen stattfindet. Die innere Grenze beider e in den Integrationen stimmt aber mit der in der säkular bestimmten Grenze überein. i und Ω werden gut durch säkulare Störungen abgebildet, die Länge des Periapsis rotiert so wie in den Integrationen, wobei sich die Rotationsgeschwindigkeit von c ändert.

Das Einfügen von masselosen Körpern zeigt, dass es einen sehr kleinen, instabilen Bereich in der inneren stabilen Zone des Systems bei 0.117 AE gibt. Stabile Zonen könnten zwischen den Körpern und außerhalb existieren, jedoch führen andere Effekte zur Destabilisierung, da in den Integrationen nichts bestehen blieb. In den anderen stabilen Bereichen liegt die durch die massiven Planeten erzwungene Exzentrizität bei nahezu null, während die erzwungene Inklination ungefähr den Wert von c annimmt. Ebenso verhalten sich das Argument des Knotens und die Länge des Periapsis. Bei der letzteren spielt diese Anregung aber nur eine untergeordnete Rolle, da die massiven Planeten rotieren.

Im System HD 40307 befinden sich drei Planeten mit Massen zwischen 0.0132 und 0.0288 Jupitermassen in sehr nahen Orbits um den Zentralstern. Durchgeführte Integrationen zeigten, dass die Stabilität der massiven Planeten gegeben ist, wobei die Bahnänderungen nahezu null sind. Die kreisförmigen Orbits werden jedoch sehr leicht elliptisch. Da die anderen Elemente gleich sind, ändert sich bei ihnen nichts.

Probekörper wurden in Distanzen von 0.02 bis 10.0 AE eingefügt, die Exzentrizität wurde in den meisten Fällen auf drei verschiedene Werte, nämlich null, 0.05 und 0.10 gestellt, es wurden aber teilweise auch andere e getestet. Stabilität ist im allgemeine für fast alle Testkörper gegeben, die einzigen Einschränkungen gibt es bei Startwerten in a, die sehr nahe an den massiven Planeten liegen, insbesondere für höhere e.

Instabilität besteht auch für gewisse Bahnresonanzen, sogar auf kreisförmigen Orbits. Die meisten Bahnresonanzen sind aber stabil, sogar mit e von 0.05 oder 0.10. Gefunden wurde in dieser Arbeit auch, dass Körper im L4 zweier massiver Planeten auf regulären Orbits bleiben , für Planet d sogar mit e von bis zu 0.10. Eine Laplace-Resonanz ist ebenfalls möglich, nämlich zwischen d und Körper in äußeren Bahnresonanzen. Bei Planet c ist keine solche Resonanz möglich. Sind Testkörper stabil, bleiben die Abweichungen in a und e nahezu null. Dies schließt die im Zusammenhang mit dieser Arbeit betriebenen Untersuchungen ab. Das Studium von extrasolaren Systemen mit mehreren Planeten wird jedoch in der Zukunft ein wichtiges Gebiet der Astrophysik bleiben, da die Formation von mehr als einem Körper in den meisten Fällen wahrscheinlich ist.

65

7 Appendix

7.1 HD 60532 - Results of tests with 0° inclination

The following tables show the results of the tests of HD 60532, with the test bodies having an eccentricity of 0° inclination with respect to the plane of the sky. The tables are again separated into the three sections, as well as one with the 1:1 mean motion resonance. The columns are semi-major axis in AU (a), eccentricity (e), time of simulation, or in case of ejection, time until escape, in 1000 years (t) and whether the object was still in the system at the end of the test (E?). If there were several testsc in the same configuration, and the longer one was not stable but the shorter one was, both are mentioned.

Inner section

a	e	t	E?	a	e	t	E?	a	e	t	E?
0.100	0.00-0.10	<= 100	y	0.200	0.07	<= 100	y	0.338	0.01	<= 50	n
0.114	0.00-0.10	<= 100	y	0.200	0.07	736	n	0.338	0.02	<= 20	n
0.123	0.00-0.10	1000	y	0.200	0.08	<= 100	y	0.338	0.03	<= 100	n
0.136	0.00-0.10	<= 100	y	0.200	0.08	682	n	0.338	0.04	<= 20	n
0.158	0.00-0.10	450	y	0.200	0.09	694	n	0.338	0.05	<= 50	n
0.180	0.00-0.10	<= 100	y	0.200	0.09	<= 100	y	0.338	0.06-0.10	<= 20	n
0.200	0.00	872	y	0.200	0.10	<= 100	y	0.342	0.00-0.10	<= 5	n
0.200	0.01	<= 100	y	0.200	0.10	804	n	0.397	0.00-0.10	<= 1	n
0.200	0.01	809	n	0.269	0.00	<= 50	n	0.406	0.00-0.10	<= 1	n
0.200	0.02	815	n	0.269	0.01	<= 50	n	0.475	0.00-0.10	<= 1	n
0.200	0.02	<= 100	y	0.269	0.03	324	n	0.481	0.00-0.10	<= 1	n
0.200	0.03	872	y	0.269	0.05	<= 100	n	0.544	0.00-0.10	<= 1	n
0.200	0.04	872	y	0.269	0.07	187	n	0.613	0.00-0.10	<= 1	n
0.200	0.05	<= 100	y	0.269	0.09	<= 50	n	0.630	0.00-0.10	<= 1	n
0.200	0.05	695	n	0.269	0.10	789	n	0.681	0.00-0.10	<= 1	n
0.200	0.06	1000	y	0.338	0.00	<= 20	n	0.750	0.00-0.10	<= 1	n

Middle section

a	e	t	E?	a	e	t	E?	a	e	t	E?
0.950	0.00-0.10	<= 1	n	1.050	0.00	<= 20	n	1.250	0.00-0.10	<= 5	n
1.000	0.00	<= 5	n	1.050	0.01-0.09	<= 5	n	1.300	0.00-0.10	<= 5	n
1.000	0.01	<= 1	n	1.050	0.10	<= 20	n	1.350	0.00	<= 5	n
1.000	0.02	<= 1	n	1.100	0.00-0.09	<= 5	n	1.350	0.01	<= 5	n
1.000	0.03	<= 5	n	1.100	0.10	<= 20	n	1.350	0.02	<= 20	n
1.000	0.04	<= 5	n	1.150	0.00	<= 20	n	1.350	0.03-0.10	<= 20	n
1.000	0.05	<= 1	n	1.150	0.01-0.08	<= 5	n	1.400	0.00-0.07	<= 5	n
1.000	0.06	<= 5	n	1.150	0.09	<= 20	n	1.400	0.08	<= 20	n
1.000	0.07	<= 5	n	1.150	0.10	<= 5	n	1.400	0.09	<= 5	n
1.000	0.08	<= 1	n	1.200	0.00-0.03	<= 5	n	1.400	0.10	<= 5	n
1.000	0.09	<= 5	n	1.200	0.04	<= 20	n	1.550	0.00-0.10	<= 1	n
1.000	0.10	<= 5	n	1.200	0.05-0.10	<= 5	n				

Outer section

a	e	t	E?	a	e	t	E?	a	e	t	E?
1.587	0.00-0.10	<= 5	n	3.640	0.09	418	n	4.620	0.07	890	n
1.600	0.00-0.10	<= 5	n	3.640	0.10	494	n	4.620	0.08	1000	y
1.700	0.00-0.10	<= 1	n	3.980	0.00	385	n	4.620	0.09	1000	y
1.940	0.00-0.10	<= 5	n	3.980	0.01	386	n	4.620	0.10	1000	y
2.080	0.00-0.10	<= 5	n	3.980	0.02	375	n	4.660	0.00-0.04	1000	y
2.280	0.00-0.10	<= 5	n	3.980	0.03	1000	y	4.660	0.05	549	n
2.520	0.00-0.10	<= 5	n	3.980	0.04	729	n	4.660	0.06-0.09	1000	y
2.620	0.00-0.10	<= 5	n	3.980	0.05-0.08	1000	y	4.660	0.10	647	n
2.924	0.00-0.10	<= 5	n	3.980	0.09	366	n	5.000	0.00-0.10	1000	y
2.960	0.00-0.10	<= 50	n	3.980	0.10	346	n	6.000	0.00-0.10	1000	y
3.300	0.00-0.10	<= 50	n	4.320	0.00	1000	y	7.000	0.00-0.10	<= 100	y
3.640	0.00	277	n	4.320	0.01	772	n	8.000	0.00-0.10	<= 100	y
3.640	0.01	1000	y	4.320	0.02-0.10	1000	y	9.000	0.00-0.10	<= 100	y
3.640	0.02	528	n	4.620	0.00	980	n	10.000	0.00-0.10	<= 100	y
3.640	0.03	433	n	4.620	0.01	1000	y	11.000	0.00-0.10	<= 100	y
3.640	0.04	171	n	4.620	0.02	957	n	12.000	0.00-0.10	<= 100	y
3.640	0.05	320	n	4.620	0.03	1000	y	13.000	0.00-0.10	<= 100	y
3.640	0.06	538	n	4.620	0.04	1000	y	14.000	0.00	<= 100	y
3.640	0.07	521	n	4.620	0.05	925	n				
3.640	0.08	854	n	4.620	0.06	1000	y				

1:1 Mean motion resonance

The double mentioning of both planets is due to placing the test bodies in L4 and L5.

a	e	t	E?	a	e	t	E?	a	e	t	E?
0.770	0.000	<= 5	n	0.770	0.278	<= 1	n	1.580	0.038	<= 5	n
0.770	0.000	<= 5	n	1.580	0.000	<= 1	n	1.580	0.038	<= 1	n
0.770	0.278	<= 1	n	1.580	0.000	<= 5	n				

7.2   HD 60532 - Results of tests with 5° inclination

Results of the systems with an inclination of 5° with respect to the plane of the sky. Abbrevitations are the same with the same units as in section 7.1.

Inner section

a	e	t	E?	a	e	t	E?	a	e	t	E?
0.123	0.00-0.03	642	y	0.406	0.04	<= 10	n	0.613	0.02	<= 10	n
0.123	0.05	589	y	0.406	0.05	<= 5	n	0.613	0.03	<= 10	n
0.123	0.08-0.10	589	y	0.406	0.06	<= 5	n	0.613	0.04-0.06	<= 5	n
0.130	0.00	1000	y	0.406	0.07-0.10	<= 10	n	0.613	0.07	<= 10	n
0.130	0.04	1000	y	0.475	0.00-0.03	<= 5	n	0.613	0.08-0.10	<= 5	n
0.130	0.07	1000	y	0.475	0.04	<= 10	n	0.681	0.00-0.02	<= 5	n
0.130	0.10	1000	y	0.475	0.05	<= 10	n	0.681	0.03	<= 10	n
0.200	0.00-0.10	1000	y	0.475	0.06	<= 20	n	0.681	0.04	<= 10	n
0.338	0.00	<= 5	n	0.475	0.07	<= 5	n	0.681	0.05	<= 20	n
0.338	0.01	<= 10	n	0.475	0.08	<= 5	n	0.681	0.06-0.09	<= 5	n
0.338	0.02	<= 5	n	0.475	0.09	<= 10	n	0.681	0.10	<= 20	n
0.338	0.03	<= 20	n	0.475	0.10	<= 5	n	0.750	0.00	<= 5	n
0.338	0.04	<= 10	n	0.544	0.00-0.03	<= 5	n	0.750	0.01	<= 5	n
0.338	0.05	<= 5	n	0.544	0.04	<= 20	n	0.750	0.02	<= 10	n
0.338	0.06-0.09	<= 10	n	0.544	0.05	<= 5	n	0.750	0.03-0.05	<= 5	n
0.338	0.10	<= 20	n	0.544	0.06-0.08	<= 10	n	0.750	0.06	<= 10	n
0.350	0.00-0.10	<= 1	n	0.544	0.09	<= 5	n	0.750	0.07	<= 5	n
0.406	0.00	<= 10	n	0.544	0.10	<= 20	n	0.750	0.08	<= 10	n
0.406	0.01	<= 10	n	0.600	0.00-0.10	<= 1	n	0.750	0.09	<= 5	n
0.406	0.02	<= 20	n	0.613	0.00	<= 5	n	0.750	0.10	<= 5	n
0.406	0.03	<= 10	n	0.613	0.01	<= 5	n				

Middle section

a	e	t	E?	a	e	t	E?	a	e	t	E?
0.800	0.00-0.10	<= 5	n	1.150	0.00-0.10	<= 5	n	1.500	0.00-0.10	<= 5	n
0.975	0.00-0.10	<= 5	n	1.325	0.00-0.10	<= 5	n				

Outer section

a	e	t	E?	a	e	t	E?	a	e	t	E?
1.700	0.00-0.05	<= 10	n	3.586	0.02	700	n	4.057	0.00-0.05	150	n
1.700	0.06-0.10	<= 5	n	3.586	0.03	760	n	4.057	0.06	800	n
2.171	0.00-0.05	<= 10	n	3.586	0.04	370	n	4.057	0.07	300	n
2.171	0.06-0.10	<= 5	n	3.586	0.05	1000	y	4.057	0.08	170	n
2.643	0.00-0.05	<= 10	n	3.586	0.06	<= 100	n	4.057	0.09	300	n
2.643	0.06-0.10	<= 5	n	3.586	0.07	500	n	4.057	0.10	170	n
3.114	0.00-0.10	<= 100	n	3.586	0.08	800	n	4.529	0.00-0.10	1000	y
3.586	0.00	335	n	3.586	0.09	190	n	5.000	0.00-0.10	1000	y
3.586	0.01	335	n	3.586	0.10	630	n	6.000	0.00-0.10	1000	y

7.3　HD 60532 - Results of tests with 20° inclination

Results of the integrations with test planets having an inclination of 20° with respect to the plane of the sky. Table variables are the same as in section 7.1.

Inner section

a	e	t	E?	a	e	t	E?	a	e	t	E?
0.123	0.00	970	y	0.200	0.04	447	y	0.475	0.00-0.09	<= 5	n
0.123	0.03	1000	y	0.200	0.04	500	n	0.475	0.08	<= 50	n
0.123	0.05	970	y	0.200	0.05	1000	y	0.475	0.09	<= 5	n
0.123	0.07	1000	y	0.200	0.06	1000	y	0.475	0.10	<= 5	n
0.123	0.09	1000	y	0.200	0.07	435	n	0.544	0.00	<= 5	n
0.123	0.10	970	y	0.200	0.08	1000	y	0.544	0.01	<= 10	n
0.200	0.00	447	y	0.200	0.09	1000	y	0.544	0.02-0.10	<= 5	n
0.200	0.00	480	n	0.200	0.10	447	y	0.613	0.00-0.04	<= 5	n
0.200	0.01	447	y	0.200	0.10	671	n	0.613	0.05	<= 10	n
0.200	0.01	689	n	0.338	0.00-0.09	<= 5	n	0.613	0.06-0.10	<= 5	n
0.200	0.02	447	y	0.338	0.10	<= 20	n	0.681	0.00-0.10	<= 5	n
0.200	0.02	500	n	0.406	0.00-0.08	<= 5	n	0.750	0.00-0.08	<= 5	n
0.200	0.03	447	y	0.406	0.09	<= 10	n	0.750	0.09	<= 10	n
0.200	0.03	470	n	0.406	0.10	<= 5	n	0.750	0.10	<= 5	n

Middle section

a	e	t	E?	a	e	t	E?	a	e	t	E?
0.800	0.00-0.10	<= 5	n	0.975	0.10	<= 5	n	1.500	0.00-0.10	<= 5	n
0.975	0.00-0.08	<= 5	n	1.150	0.00-0.10	<= 5	n				
0.975	0.09	<= 20	n	1.325	0.00-0.10	<= 5	n				

Outer section

a	e	t	E?	a	e	t	E?	a	e	t	E?
1.700	0.00	<= 1	n	2.171	0.05	<= 5	n	3.114	0.07	243	n
1.700	0.01	<= 5	n	2.171	0.06	<= 1	n	3.114	0.08-0.10	<= 100	n
1.700	0.02	<= 5	n	2.171	0.07-0.10	<= 10	n	3.586	0.00	1000	y
1.700	0.03	<= 10	n	2.643	0.00	<= 10	n	3.586	0.01	322	n
1.700	0.04	<= 1	n	2.643	0.01-0.04	<= 5	n	3.586	0.02	1000	y
1.700	0.05	<= 5	n	2.643	0.05	<= 1	n	3.586	0.03	474	n
1.700	0.06	<= 1	n	2.643	0.06	<= 10	n	3.586	0.04	566	n
1.700	0.07	<= 1	n	2.643	0.07	<= 20	n	3.586	0.05	320	n
1.700	0.08	<= 10	n	2.643	0.08-0.10	<= 10	n	3.586	0.06	191	n
1.700	0.09	<= 1	n	3.114	0.00	105	n	3.586	0.07	272	n
1.700	0.10	<= 1	n	3.114	0.01	<= 100	n	3.586	0.08	268	n
2.171	0.00	<= 10	n	3.114	0.02	105	n	3.586	0.09	296	n
2.171	0.01	<= 5	n	3.114	0.03	105	n	3.586	0.10	432	n
2.171	0.02	<= 10	n	3.114	0.04	<= 100	n	5.000	0.00-0.10	1000	y
2.171	0.03	<= 1	n	3.114	0.05	105	n	6.000	0.00-0.10	1000	y
2.171	0.04	<= 5	n	3.114	0.06	243	n				

Mean motion resonances

The mean motion resonances with both massive planets. In the 1:1 resonance, all test bodies were placed in L4 and L5, thus the double mentioning.

a	e	t	E?	a	e	t	E?	a	e	t	E?
0.233	0.00-0.02	<= 10	n	0.485	0.02-0.04	<= 5	n	1.602	0.08	<= 5	n
0.233	0.03	<= 5	n	0.485	0.05-0.06	<= 1	n	1.602	0.09	<= 1	n
0.233	0.04	<= 20	n	0.485	0.07-0.08	<= 5	n	1.602	0.10	<= 5	n
0.233	0.05	<= 5	n	0.485	0.09	<= 1	n	1.940	0.00-0.01	<= 1	n
0.233	0.06	<= 100	n	0.485	0.10	<= 10	n	1.940	0.02	<= 10	n
0.233	0.07	<= 20	n	0.540	0.00-0.10	<= 1	n	1.940	0.03	<= 5	n
0.233	0.08-0.09	<= 10	n	0.627	0.00-0.10	<= 1	n	1.940	0.04-0.05	<= 1	n
0.233	0.10	<= 100	n	0.760	0.00-0.10	<= 1	n	1.940	0.06-0.08	<= 5	n
0.263	0.00-0.02	<= 10	n	0.770	0.00-0.10	<= 1	n	1.940	0.09-0.10	<= 1	n
0.263	0.03	<= 5	n	0.770	0.00-0.10	<= 1	n	2.251	0.00-0.01	<= 5	n
0.263	0.04	<= 20	n	0.770	0.278	<= 1	n	2.251	0.02	<= 1	n
0.263	0.05	<= 5	n	0.770	0.278	<= 1	n	2.251	0.03-0.04	<= 10	n
0.263	0.06	<= 10	n	0.995	0.00-0.10	<= 1	n	2.251	0.05-0.06	<= 5	n
0.263	0.07	<= 50	n	1.222	0.00-0.03	<= 1	n	2.251	0.07	<= 10	n
0.263	0.08-0.09	<= 5	n	1.222	0.04	<= 10	n	2.251	0.08	<= 5	n
0.263	0.10	<= 10	n	1.222	0.05-0.06	<= 1	n	2.251	0.09-0.10	<= 1	n
0.306	0.00	<= 5	n	1.222	0.07	<= 10	n	2.508	0.00-0.10	<= 5	n
0.306	0.01	<= 10	n	1.222	0.08-0.09	<= 1	n	2.542	0.00-0.01	<= 1	n
0.306	0.02-0.06	<= 5	n	1.222	0.10	<= 5	n	2.542	0.02	<= 5	n
0.306	0.07-0.09	<= 10	n	1.580	0.00-0.10	<= 1	n	2.542	0.03-0.04	<= 1	n
0.306	0.10	<= 20	n	1.580	0.00-0.10	<= 1	n	2.542	0.05-0.06	<= 5	n
0.370	0.00-0.03	<= 5	n	1.580	0.038	<= 1	n	2.542	0.07	<= 10	n
0.370	0.04-0.05	<= 10	n	1.580	0.038	<= 1	n	2.542	0.08-0.10	<= 1	n
0.370	0.06-0.09	<= 5	n	1.602	0.00-0.03	<= 1	n	3.287	0.00-0.10	273	n
0.370	0.10	<= 10	n	1.602	0.04	<= 5	n	3.981	0.00-0.10	489	n
0.479	0.00-0.10	<= 1	n	1.602	0.05	<= 1	n	4.620	0.00-0.06	1000	y
0.485	0.00	<= 10	n	1.602	0.06	<= 5	n	4.620	0.07	950	n
0.485	0.01	<= 10	n	1.602	0.07	<= 1	n	4.620	0.08-0.10	1000	y

7.4   HD 60532 - Results of tests with 25° inclination

Test planets with an inclination of 25° with respect to the plane of the sky. Tabular parameters are the same as in section 7.1.

Inner section

a	e	t	E?	a	e	t	E?	a	e	t	E?
0.100	0.00-0.10	<= 100	y	0.406	0.01	<= 1	n	0.613	0.00	<= 1	n
0.123	0.00-0.10	1000	y	0.406	0.02-0.04	<= 10	n	0.613	0.01	<= 50	n
0.133	0.00-0.10	<= 100	y	0.406	0.05	<= 1	n	0.613	0.02	<= 1	n
0.167	0.00-0.10	<= 100	y	0.406	0.06	<= 20	n	0.613	0.03	<= 1	n
0.200	0.00	744	n	0.406	0.07	<= 1	n	0.613	0.04	<= 10	n
0.200	0.01	1000	y	0.406	0.08	<= 10	n	0.613	0.05	<= 1	n
0.200	0.02	761	n	0.406	0.09	<= 1	n	0.613	0.06	<= 1	n
0.200	0.03	744	n	0.406	0.10	<= 1	n	0.613	0.07	<= 10	n
0.200	0.04	1000	y	0.475	0.00	<= 1	n	0.613	0.08-0.10	<= 1	n
0.200	0.05	580	n	0.475	0.01	<= 1	n	0.681	0.00-0.06	<= 1	n
0.200	0.06	938	n	0.475	0.02	<= 10	n	0.681	0.07	<= 10	n
0.200	0.07	722	n	0.475	0.03	<= 1	n	0.681	0.08	<= 1	n
0.200	0.08	932	n	0.475	0.04	<= 10	n	0.681	0.09	<= 1	n
0.200	0.09	904	n	0.475	0.05	<= 10	n	0.681	0.10	<= 10	n
0.200	0.10	825	n	0.475	0.06-0.08	<= 1	n	0.750	0.00	<= 10	n
0.338	0.00	<= 10	n	0.475	0.09	<= 10	n	0.750	0.01	<= 10	n
0.338	0.01	<= 10	n	0.475	0.10	<= 1	n	0.750	0.02-0.05	<= 1	n
0.338	0.02	<= 20	n	0.544	0.00	<= 20	n	0.750	0.06	<= 20	n
0.338	0.03	<= 50	n	0.544	0.01	<= 20	n	0.750	0.07	<= 1	n
0.338	0.04-0.07	<= 10	n	0.544	0.02-0.04	<= 1	n	0.750	0.08	<= 10	n
0.338	0.08	<= 1	n	0.544	0.05	<= 20	n	0.750	0.09	<= 1	n
0.338	0.09	<= 20	n	0.544	0.06-0.08	<= 1	n	0.750	0.10	<= 1	n
0.338	0.10	<= 1	n	0.544	0.09	<= 10	n				
0.406	0.00	<= 10	n	0.544	0.10	<= 10	n				

Middle section

a	e	t	E?	a	e	t	E?	a	e	t	E?
0.800	0.00-0.10	<= 5	n	1.150	0.00-0.10	<= 5	n	1.500	0.00-0.10	<= 5	n
0.975	0.00-0.10	<= 5	n	1.325	0.00-0.10	<= 5	n				

Outer section

a	e	t	E?	a	e	t	E?	a	e	t	E?
1.700	0.00-0.10	<= 5	n	3.586	0.02	214	n	4.057	0.07	270	n
2.171	0.00-0.10	<= 5	n	3.586	0.03	421	n	4.057	0.08	<= 100	n
2.643	0.00-0.10	<= 5	n	3.586	0.04	1000	y	4.057	0.09	607	n
3.114	0.00	130	n	3.586	0.05	299	n	4.057	0.10	735	n
3.114	0.01	<= 50	n	3.586	0.06	1000	y	4.529	0.00-0.06	1000	y
3.114	0.02	<= 100	n	3.586	0.07	539	n	4.529	0.07	617	n
3.114	0.03	130	n	3.586	0.08	<= 100	n	4.529	0.08	742	n
3.114	0.04	130	n	3.586	0.09	130	n	4.529	0.09	539	n
3.114	0.05	<= 100	n	3.586	0.10	180	n	4.529	0.10	1000	y
3.114	0.06	<= 50	n	4.057	0.00	539	n	5.000	0.00-0.06	1000	y
3.114	0.07	<= 50	n	4.057	0.01	130	n	5.000	0.07	539	n
3.114	0.08	<= 100	n	4.057	0.02	892	n	5.000	0.08	539	n
3.114	0.09	<= 50	n	4.057	0.03	892	n	5.000	0.09	617	n
3.114	0.10	<= 100	n	4.057	0.04	240	n	5.000	0.10	1000	y
3.586	0.00	546	n	4.057	0.05	1000	y	5.500	0.00-0.10	1000	y
3.586	0.01	546	n	4.057	0.06	421	n	6.000	0.00-0.10	1000	y

71

7.5 HD 40307 - Results

These tables show the results of the integrations of the HD 40307 system. Columns are semi-major axis in AU (a), eccentricity (e), simulation duration or, in case of instability of the planet time of escape, in 1000 years (t) and whether the planet was still stable in the system at the end of the integration (E?).

Inner/middle section

a	e	t	E?	a	e	t	E?	a	e	t	E?
0.020	0.000	1000	y	0.040	0.000	1000	y	0.054	0.100	$<= 5$	n
0.020	0.050	1000	y	0.040	0.050	1000	y	0.100	0.050	1000	y
0.020	0.100	1000	y	0.040	0.100	1000	y	0.100	0.070	200	n
0.025	0.000	401	y	0.054	0.000	1000	y	0.100	0.090	$<= 5$	n
0.025	0.050	401	y	0.054	0.020	873	y	0.100	0.080	$<= 10$	n
0.025	0.100	401	y	0.054	0.050	176	n	0.108	0.010	1000	y
0.030	0.000	312	y	0.054	0.060	$<= 50$	n	0.108	0.030	915	y
0.030	0.050	219	y	0.054	0.070	$<= 5$	n	0.108	0.100	$<= 5$	n
0.030	0.100	217	y	0.054	0.080	$<= 5$	n				

Outer section

a	e	t	E?	a	e	t	E?	a	e	t	E?
0.160	0.050	1000	y	0.442	0.020	880	y	1.000	0.030-0.090	125	y
0.160	0.070	1000	y	0.442	0.030	1000	y	1.000	0.100	1000	y
0.160	0.080	1000	n	0.442	0.040	695	y	1.080	0.000	549	y
0.160	0.090	103	n	0.442	0.080	1000	y	3.250	0.000-0.100	$<= 50$	y
0.160	0.095	1000	n	0.442	0.090	772	y	5.500	0.000-0.100	$<= 50$	y
0.160	0.100	377	n	1.000	0.000	1000	y	7.750	0.000-0.100	$<= 50$	y
0.170	0.070	1000	y	1.000	0.010	125	y	10.000	0.000-0.100	$<= 50$	y
0.200	0.000	1000	y	1.000	0.020	$<= 50$	y				

Mean motion resonance

a	e	t	E?	a	e	t	E?	a	e	t	E?
0.041	0.000	1000	y	0.129	0.000	$<= 5$	n	0.279	0.100	1000	y
0.041	0.050	1000	y	0.134	0.000	1000	y	0.338	0.000	1000	y
0.046	0.000	$<= 5$	n	0.134	0.050	1000	y	0.338	0.050	1000	y
0.046	0.050	$<= 5$	n	0.134	0.100	1000	y	0.338	0.100	1000	y
0.053	0.000	1000	y	0.168	0.000	1000	y	0.392	0.000	1000	y
0.053	0.050	$<= 5$	n	0.204	0.000	1000	y	0.392	0.050	1000	y
0.064	0.000	1000	y	0.213	0.000	1000	y	0.392	0.100	1000	y
0.064	0.050	1000	y	0.213	0.050	1000	y	0.442	0.000	1000	y
0.081	0.000	1000	y	0.213	0.100	1000	y	0.442	0.010	862	y
0.084	0.000	$<= 1$	n	0.279	0.000	1000	y	0.442	0.050	1000	y
0.084	0.050	$<= 1$	n	0.279	0.050	1000	y	0.442	0.100	1000	y

7.6 Mathematica calculations

Mathematica calculation of the secular perturbation

Wolfram *Mathematica* notebook for the calculation of secular resonences by two bodies orbiting a point mass object.
Author: Simon Rothwangl
Date: 01/03/2010
This notebook uses a package done by F. Zugno for the calculation of the Laplace coefficients, which can be downloaded from
http://library.wolfram.com/infocenter/MathSource/4256

■ Perturbations of the massive Planets

■ Planet Data

Input: mi in kg, ai in AU; omi, i, Gom in degree.
The central star is considered point mass.

```
Clear["Global`*"];
m1 = 3.15 * 1.9 * 10^27;
m2 = 7.46 * 1.9 * 10^27;
ms = 1.44 * 1.99 * 10^30;
m1 = m1 / ms
m2 = m2 / ms
ms = 1;
a1 = 0.77;
a2 = 1.58;
e1 = 0.278;
e2 = 0.038;
om1 = 352.83;
om2 = 119.49;
i1 = 1.5;
i2 = 2.5;
Gom1 = 20.0;
Gom2 = 30.0;
n1 = 360 ( a1^(3/2));
n2 = 360 ( a2^(3/2));
α12 = a1 / a2
```

```
0.00208857

0.00494626

0.487342
```

■ Laplace Coefficients

```
<< Perturbations`LaplaceCoefficients`
```

SetDelayed::write : Tag LaplaceCoefficient in LaplaceCoefficient[s_, j_?Negative, p_, al_] is Protected.

SetDelayed::write : Tag LaplaceCoefficient in LaplaceCoefficient[s_, j_, 0, al_] is Protected.

SetDelayed::write : Tag LaplaceCoefficient in LaplaceCoefficient[s_, j_, p_, al_] is Protected.

General::stop : Further output of SetDelayed::write will be suppressed during this calculation.

```
LaplaceCoefficient[3 / 2, 1, 0, 0.1]
```

0.305708

```
b1 = LaplaceCoefficient[3 / 2, 1, 0, α12]
b2 = LaplaceCoefficient[3 / 2, 2, 0, α12]
```

2.43759

1.43722

■ Matrix elements of the disturbing functions

$$A = \begin{pmatrix} (n1 / 4) * (m2 (ms + m1)) * (α12 * α12) * b1 & - (n1 / 4) * (m2 (ms + m1)) * α12 * α12 * b2 \\ - (n2 / 4) * (m1 (ms + m2)) * α12 * b2 & (n2 / 4) * (m1 (ms + m2)) * α12 * b1 \end{pmatrix}$$

{{0.380633, -0.224423}, {-0.0659659, 0.111881}}

$$B = \begin{pmatrix} - (n1 / 4) * (m2 (ms + m1)) * (α12 * α12) * b1 & (n1 / 4) * (m2 (ms + m1)) * α12 * α12 * b1 \\ (n2 / 4) * (m1 (ms + m2)) * α12 * b1 & - (n2 / 4) * (m1 (ms + m2)) * α12 * b1 \end{pmatrix}$$

{{-0.380633, 0.380633}, {0.111881, -0.111881}}

■ Eigenvalues of A and B

```
{g2, g1} = Eigenvalues[A]
```

{0.427533, 0.0649807}

```
{f2, f1} = Eigenvalues[B]
```

$\{-0.492514, -1.2055 \times 10^{-17}\}$

■ Unscaled Eigenvektors

```
{ex1, ex2} = Eigenvectors[A]
```

{{0.978853, -0.204564}, {0.579455, 0.815005}}

```
{e12, e22} = ex1;
{e11, e21} = ex2;
e11
e21
```

```
0.579455
```

```
0.815005
```

```
{in1, in2} = Eigenvectors[B]
```

```
{{-0.959413, 0.282005}, {-0.707107, -0.707107}}
```

```
{i12, i22} = in1;
{i11, i21} = in2;
i12
i22
```

```
-0.959413
```

```
0.282005
```

■ Determining the scaling factors

New variables at t=0

```
h = {e1 * Sin[om1 / 180 * π], e2 * Sin[om2 / 180 * π]}
k = {e1 * Cos[om1 / 180 * π], e2 * Cos[om2 / 180 * π]}
p = {i1 / 180 * π * Sin[Gom1 / 180 * π], i2 / 180 * π * Sin[Gom2 / 180 * π]}
q = {i1 / 180 * π * Cos[Gom1 / 180 * π], i2 / 180 * π * Cos[Gom2 / 180 * π]}
```

```
{-0.0346982, 0.0330768}
```

```
{0.275826, -0.0187063}
```

```
{0.00895407, 0.0218166}
```

```
{0.0246011, 0.0377875}
```

```
matrixe = {{e11, e12}, {e21, e22}};
matrixi = {{i11, i12}, {i21, i22}};
{S1sin, S2sin} = LinearSolve[matrixe, h]
{S1cos, S2cos} = LinearSolve[matrixe, k]
{T1sin, T2sin} = LinearSolve[matrixi, p]
{T1cos, T2cos} = LinearSolve[matrixi, q]
```

```
{0.0275883, -0.0517794}
```

```
{0.0415945, 0.257162}
```

```
{-0.0267212, 0.0103612}
```

```
{-0.0492033, 0.010622}
```

```
S1 = Sqrt[S1sin^2 + S1cos^2]
S2 = Sqrt[S2sin^2 + S2cos^2]
β1 = ArcCos[S1cos / S1];
β2 = ArcCos[S2cos / S2];
β1 * 180 / π
β2 * 180 / π
T1 = Sqrt[T1sin^2 + T1cos^2]
T2 = Sqrt[T2sin^2 + T2cos^2]
γ1 = ArcCos[T1cos / T1];
γ2 = ArcCos[T2cos / T2];
γ1 * 180 / π
γ2 * 180 / π
```

0.0499121

0.262323

−29.4743

15.4648

0.055991

0.0148385

151.495

−44.2877

■ Scaled Eigenvectors

```
e11 = e11 * S1
e21 = e21 * S1
e12 = e12 * S2
e22 = e22 * S2
i11 = i11 * T1
i21 = i21 * T1
i12 = i12 * T2
i22 = i22 * T2
```

0.0289218

0.0406786

0.256776

−0.0536618

−0.0395916

−0.0395916

−0.0142363

0.00418454

- **New variables with scaled eigenvectors**

```
h1n[x_] = e11 * Sin[g1 * (π / 180) * x + β1] + e12 * Sin[g2 * (π / 180) * x + β2];
h2n[x_] = e21 * Sin[g1 * (π / 180) * x + β1] + e22 * Sin[g2 * (π / 180) * x + β2];
k1n[x_] = e11 * Cos[g1 * (π / 180) * x + β1] + e12 * Cos[g2 * (π / 180) * x + β2];
k2n[x_] = e21 * Cos[g1 * (π / 180) * x + β1] + e22 * Cos[g2 * (π / 180) * x + β2];
p1n[x_] = i11 * Sin[f1 * (π / 180) * x + γ1] + i12 * Sin[f2 * (π / 180) * x + γ2];
p2n[x_] = i21 * Sin[f1 * (π / 180) * x + γ1] + i22 * Sin[f2 * (π / 180) * x + γ2];
q1n[x_] = i11 * Cos[f1 * (π / 180) * x + γ1] + i12 * Cos[f2 * (π / 180) * x + γ2];
q2n[x_] = i21 * Cos[f1 * (π / 180) * x + γ1] + i22 * Cos[f2 * (π / 180) * x + γ2];
```

- **Variations of eccentricity and inclination for the massive planets**

Time units are yrs, angles in degrees.

```
eccentricity1[x_] = Sqrt[h1n[x]^2 + k1n[x]^2];
eccentricity2[x_] = Sqrt[h2n[x]^2 + k2n[x]^2];
Plot[{eccentricity1[x], eccentricity2[x]}, {x, -1000, 1000},
  PlotStyle → {{RGBColor[1, 0, 0]}, {RGBColor[0, 0, 1]}}];

omega1[x_] = ArcCos[k1n[x]  eccentricity1[x]] * 180 / π;
omega2[x_] = ArcCos[k2n[x]  eccentricity2[x]] * 180 / π;
Plot[{omega1[x], omega2[x]}, {x, -2000, 2000},
  PlotStyle → {{RGBColor[1, 0, 0]}, {RGBColor[0, 0, 1]}}];
```

Using 2 branches of ArcCos in case of rotating om, therefore solution in next graph.

```
omega21n[x_] := If[omega2'[x] > 0, 360 - ArcCos[k2n[x]  eccentricity2[x]] * 180 / Pi,];
omega22n[x_] := If[omega2'[x] < 0, ArcCos[k2n[x]  eccentricity2[x]] * 180 / Pi,];
omega11n[x_] := If[omega1'[x] > 0, 360 - ArcCos[k1n[x]  eccentricity1[x]] * 180 / Pi,];
omega12n[x_] := If[omega1'[x] < 0, ArcCos[k1n[x]  eccentricity1[x]] * 180 / Pi,];
Plot[{omega21n[x], omega22n[x], omega11n[x], omega12n[x]},
  {x, 0, 5000}, PlotStyle → {{RGBColor[0, 0, 1]},
    {RGBColor[0, 0, 1]}, {RGBColor[1, 0, 0]}, {RGBColor[1, 0, 0]}}];

inclination1[x_] = Sqrt[p1n[x]^2 + q1n[x]^2] * 180 / π;
inclination2[x_] = Sqrt[p2n[x]^2 + q2n[x]^2] * 180 / π;
Plot[{inclination1[x], inclination2[x]}, {x, -1000, 1000},
  PlotStyle → {{RGBColor[1, 0, 0]}, {RGBColor[0, 0, 1]}}, PlotRange → {0, 4}];

Gomega1[x_] = ArcCos[q1n[x] ( inclination1[x] * π / 180)] * 180 / π;
Gomega2[x_] = ArcCos[q2n[x] ( inclination2[x] * π / 180)] * 180 / π;
Plot[{Gomega1[x], Gomega2[x]}, {x, -1000, 1000},
  PlotStyle → {{RGBColor[1, 0, 0]}, {RGBColor[0, 0, 1]}}];
```

- **Frequencies written out explicitly**

```
Plot[{eccentricity1[x],
  Sqrt[e11^2 + e12^2 + 2 * e11 * e12 * Cos[(g1 - g2) * (π / 180) * x + β1 - β2]]},
  {x, -1000, 1000}, PlotRange → {0, 0.3},
  PlotStyle → {{RGBColor[1, 0, 0]}, {RGBColor[0, 0, 1]}}];
```

As one can see, both plots overlap completely

Written in the form as in the plot above
all angles in degrees

Eccentricity

e of planet 1

```
e11^2 + e12^2
```
0.0667703

```
2 * e11 * e12
```
0.0148528

```
g1 - g2
```
-0.362553

```
(β1 - β2) * 180 / Pi
```
-44.9391

e of planet 2

```
e21^2 + e22^2
```
0.00453434

```
2 * e21 * e22
```
-0.00436578

```
g1 - g2
```
-0.362553

```
(β1 - β2) * 180 / Pi
```
-44.9391

Period

```
360 ( -g1 + g2)
```
992.96

Inclination

```
Plot[{inclination1[x],
    Sqrt[i11^2 + i12^2 + 2 * i11 * i12 * Cos[(f1 - f2) * (π / 180) * x + γ1 - γ2]] * (180 / π)},
   {x, -1000, 1000}, PlotRange → {0, 4},
   PlotStyle → {{RGBColor[1, 0, 0]}, {RGBColor[0, 0, 1]}}];
```

i of planet 1

```
i11^2 + i12^2
```
0.00177017

```
2 * i11 * i12
```

0.00112727

```
f1 - f2
```

0.492514

```
(γ1 - γ2) * 180 / Pi
```

195.782

i of planet 2

```
i21 ^ 2 + i22 ^ 2
```

0.001585

```
2 * i21 * i22
```

-0.000331345

```
f1 - f2
```

0.492514

```
(γ1 - γ2) * 180 / Pi
```

195.782

Period

```
360 ( -f1 + f2)
```

-730.944

Test particle

Time units are yrs, angles in degrees.

■ **Determining Elements A and B of the disturbing function**

```
erster[a_] := If[a1 < a, (a1 / a) * LaplaceCoefficient[3 / 2, 1, 0, a1 / a],
    ((a / a1) ^ 2) * LaplaceCoefficient[3 / 2, 1, 0, a / a1]];
zweiter[a_] := If[a2 < a, (a2 / a) * LaplaceCoefficient[3 / 2, 1, 0, a2 / a],
    ((a / a2) ^ 2) * LaplaceCoefficient[3 / 2, 1, 0, a / a2]];
planetA[a_] := (360 ( a ^ (3 / 2))  4) * (m1 * erster[a] + m2 * zweiter[a]);
planetB[a_] := -planetA[a];

Plot[planetA[a], {a, 0, 20}, PlotRange → {0, 0.05}];
```

■ **Aj of the disturbing functions and new variables h0 and k0 for test particle**

```
Mx1[a_] := If[a1 < a, (a1 / a) * LaplaceCoefficient[3 / 2, 2, 0, a1 / a],
    ((a / a1) ^ 2) * LaplaceCoefficient[3 / 2, 2, 0, a / a1]];
Mx2[a_] := If[a2 < a, (a2 / a) * LaplaceCoefficient[3 / 2, 2, 0, a2 / a],
    ((a / a2) ^ 2) * LaplaceCoefficient[3 / 2, 2, 0, a / a2]];
MassA1[a_] := - (2 * π ( a^(3 / 2))  4) * m1 * Mx1[a];
MassA2[a_] := - (2 * π ( a^(3 / 2))  4) * m2 * Mx2[a];

ν1 = MassA1[a] * e11 + MassA2[a] * e21;
ν2 = MassA1[a] * e12 + MassA2[a] * e22;
h0[t_, a_] := - ((ν1 * (180 / π) ( planetA[a] - g1)) * Sin[(g1  180 * π) * t + β1]) -
    ((ν2 * (180 / π) ( planetA[a] - g2)) * Sin[(g2  180 * π) * t + β2]);
k0[t_, a_] := - ((ν1 * (180 / π) ( planetA[a] - g1)) * Cos[(g1  180 * π) * t + β1]) -
    ((ν2 * (180 / π) ( planetA[a] - g2)) * Cos[(g2  180 * π) * t + β2]);
```

■ **Forced eccentricity and longitude of pericenter**

```
eforced[t_, a_] = Sqrt[h0[t, a] ^ 2 + k0[t, a] ^ 2];
plot1 = ListPlot[{{a1, e1}, {a2, e2}}, PlotStyle → {PointSize[0.02], Hue[0.1]},
    PlotRange → {0, 0.5}, DisplayFunction → Identity];
plot2 = Plot[eforced[0, a], {a, 0, 30}, PlotRange → {0, 0.5},
    DisplayFunction → Identity];
Show[plot1, plot2, DisplayFunction → $DisplayFunction];

omforced[t_, a_] := ArcCos[k0[t, a]  eforced[t, a]];
plot3 = ListPlot[{{a1, om1}, {a2, om2}}, PlotStyle → {PointSize[0.02], Hue[0.1]},
    PlotRange → {-700, 700}, DisplayFunction → Identity];
plot4 = Plot[(omforced[0, a] * 180 / π), {a, 0, 4},
    PlotRange → {-700, 700}, DisplayFunction → Identity];
Show[plot3, plot4, DisplayFunction → $DisplayFunction];
```

■ **Bj of the disturbing function and new parameters p0 and q0 for the test particle**

```
MassB1[a_] := (2 * π ( a^(3 / 2))  4) * m1 * erster[a];
MassB2[a_] := (2 * π ( a^(3 / 2))  4) * m2 * zweiter[a];
μ1 = MassB1[a] * i11 + MassB2[a] * i21;
μ2 = MassB1[a] * i12 + MassB2[a] * i22;
p0[t_, a_] := - ((μ1 * (180 / π) ( planetB[a] - f1)) * Sin[(f1 / 180 * π) * t + γ1]) -
    ((μ2 * (180 / π) ( planetB[a] - f2)) * Sin[(f2 / 180 * π) * t + γ2]);
q0[t_, a_] := - ((μ1 * (180 / π) ( planetB[a] - f1)) * Cos[(f1 / 180 * π) * t + γ1]) -
    ((μ2 * (180 / π) ( planetB[a] - f2)) * Cos[(f2 / 180 * π) * t + γ2]);
```

■ **Forced inclination and longitude of ascending node**

```
iforced[t_, a_] := Sqrt[p0[t, a] ^ 2 + q0[t, a] ^ 2];
plot5 = ListPlot[{{a1, i1}, {a2, i2}}, PlotStyle → {PointSize[0.02], Hue[0.1]},
    PlotRange → {0, 3}, DisplayFunction → Identity];
plot6 = Plot[(iforced[0, a] * 180 / π), {a, 0, 30},
    PlotRange → {0, 3}, DisplayFunction → Identity];
Show[plot5, plot6, DisplayFunction → $DisplayFunction];
```

```
Gomforced[t_, a_] := ArcCos[q0[t, a]  iforced[t, a]];
plot7 = ListPlot[{{a1, Gom1}, {a2, Gom2}}, PlotStyle → {PointSize[0.02], Hue[0.1]},
    PlotRange → {0, 360}, DisplayFunction → Identity];
plot8 = Plot[(Gomforced[0, a] * 180 / π), {a, 0, 30},
    PlotRange → {0, 360}, DisplayFunction → Identity];
Show[plot7, plot8, DisplayFunction → $DisplayFunction];
```

7.7   Curriculum vitae

Personal Details

NAME	Simon Rothwangl, BSc
ADDRESS	Neustiftgasse 108/34
	1070 Vienna, Austria
E-MAIL	simon_rothwangl@hotmail.com
DATE OF BIRTH	23 April 1984
CITIZENSHIP	Austria

Education and Formation

07 - 11/2008	Exchange semester at the Australian National University, Canberra, Australia
10/2007 - today	Candidate for Master in Astronomy degree (MSc), University of Vienna, Austria
10/2004 - 10/2007	BSc in Astronomy, University of Vienna, Austria
09/2003 - 05/2004	Compulsory military service at the Austrian army
06/2003	School leaving exam (Matura) at the business school Grazbachgasse 71, Graz, Austria

Awards

- Joint Study Programme for student mobility
- Merit scholarship for excellent students

Publications

Solving the controversy about the astronomical significance of the rock formation "Teufelstein" in Styria, Astronomical Notes 330, No. 6, 2009

8 Acknowledgment

References

[1] Barnes, R., Jackson, B., Raymond, S.N. et al. 2009, *The HD 40307 Planetary System: Super-Earths or Mini-Neptunes?*, arXiv:0901.1698v1

[2] Desort, M., Lagrange, A.-M., Galland, F. et al. 2008, *Extrasolar planets and brown dwarfs around A-F type stars V. A planetary system found with HARPS around the F6IV-V star HD 60532*, Astronomy and Astrophysics 491 883-888

[3] Dvorak, R., Freistetter, F., Kurths, J. 2005, *Chaos and Stability in Planetary Systems*, Springer

[4] Ferraz-Mello, S. 1979, *Dynamics of the Galilean Satellites*, Universidade de São Paulo

[5] Hanslmeier, A., Dvorak, R. 1984, *Numerical integration with Lie-series*, Astronomy and Astrophysics 132 203-207

[6] Holmberg, J., Nordström, B., Andersen, J. 2007, *The Geneva-Copenhagen survey of the Solar neighbourhood II*, Astronomy and Astrophysics 475 519-537

[7] Laskar, J., Correia, A.C.M. 2009, *HD 60532, a planetary system in a 3 : 1 mean motion resonance*, Astronomy and Astrophysics 496 L5-L8

[8] Mayor, M., Udry, S. et al. 2009, *The HARPS search for southern extrasolar planets XIII. A planetary system with 3 super-Earths (4.2, 6.9, and 9.2 $M_\oplus$)*, Astronomy and Astrophysics 493 639-644

[9] Murray, C.D., Dermott, S.F. 1999, *Solar System Dynamics*, Cambridge University Press

[10] Schneider, J. 2009, Retrieved 24 June 2009, from http://www.exoplanet.eu/star.php?st=HD+60532

[11]   Schneider,   J.   2009b,   Retrieved   24   August   2009,   from
        http://www.exoplanet.eu/star.php?st=HD+40307

[12] Süli, Á., Dvorak, R., Schwarz, R. 2009, *List of multiplanetary systems*,
      Not published

[13] Zugno, F. 2002, *Disturbing Function*, Retrieved 2 December 2009, from
      http://library.wolfram.com/infocenter/MathSource/4256/